High resolution particle counting detectors with microchannel plates and their applications in materials research, astrophysics, biomedical imaging and synchrotron instrumentation

A.S. Tremsin

Space Sciences Laboratory,
University of California at Berkeley
Berkeley, CA 94720, USA

Acknowledgements

Experimental Astrophysics group, Space Sciences Laboratory, UC Berkeley, USA

__O. H. W. Siegmund__, J. V. Vallerga, J. B. McPhate, J. Hull, J. Tedesco, S. Jelinsky, C. Ertley, B. Welsh, P. Jelinsky, S. Jelinsky

Techne Instruments, Oakland, CA, USA

R. Raffanti

Lawrence Berkeley National Laboratory, Berkeley, USA

G. Lebedev, Z. Hussain, , J. -H. Guo, S. Roy, Per-Anders Glans
E. D. Bourret-Courchesne, G. A. Bizarri, D. Perrodin,
I. Khodyuk, T. Shalapska
S. Neppl, J. Mahl, O. Gessner

Nova Scientific, Inc, Sturbridge, USA (manufacturer of neutron sensitive MCPs)

W. B. Feller, P. White, B. White

Rutherford Appleton Laboratory, ISIS Facility, UK

W. Kockelmann, S. Y. Zhang, J. Kelleher, S. Kabra, D.E. Pooley, G. Burca

J-PARC Center, JAEA, Nagoya University, Japan

T. Shinohara. T. Kai, K. Oikawa

LANSCE, Los Alamos National Laboratory

S. Vogel, A. Losko, M. Mocko, M.A.M. Bourke

Paul Scherrer Institute, Switzerland

E. Lehmann, A. Kaestner, T. Panzner, P. Trtik, M. Morgano

Istituto dei Sistemi Complessi, Sesto Fiorentino (FI), Italy

F. Grazzi

University of Tenneessee

D. Penumadu

European Spallation Source Scandinavia

M. Strobl

Technical University of Denmark

S. Schmidt, M.Makowska

CONICET and Instituto Balseiro, Centro Atomico Bariloche, Argentina

J. Santisteban

Spallation Neutron Source, ORNL, USA

H. Z. Bilheux, L.J. Santodonato, J. Bilheux,

Technische Universität München, Germany

B. Schillinger, M. Schulz

Department of Geology and Environmental Earth Science, Miami University

John Rakovan

HZB, Berlin

N. Kardjilov, R. Woracek

Open University, UK

M. Fitzpatrick

Cranfield University, UK

Supriyo Ganguly

Oxford University, UK

A.M. Korsunsky

General Electric Global Research

Yan Gao

Physikalisch-Technische Bundesanstalt (PTB), Germany

V. Dangendorf, K. Tittelmeier

Univeristy of California Los Angeles

X. Michalet , R. A. Colyer, S. Weiss

ANL, Univ. Chicago, Incom, Inc. MA, USA

LAPPD collaboration

Arradiance, Sudbury, MA, USA

D.R. Beaulieu, D. Gorelikov, H. Klotzsch, K. Stenton, P. de Rouffignac, N. Sullivan

Colleagues I forgot.......(with my apologies)

Outline

- Overview of particle counting detectors with Microchannel Plates and their unique capabilities
  - Resolution
  - Detection efficiency
  - Counting rate capabilities
  - Developments in manufacturing technology

- Applications of MCP detectors
  - Astrophysics
  - Materials research and non-destructive testing with neutrons
  - Bioimaging
  - Synchrotron Instrumentation

MCP detector applications

- Image intensified applications
- Mass spectroscopy
- Astrophysics
- Synchrotron instrumentation
- Biomedical research (FLIM, FRET,…)
- X-Ray and UV photon detection
- Neutron radiography/ tomography and spectroscopic imaging

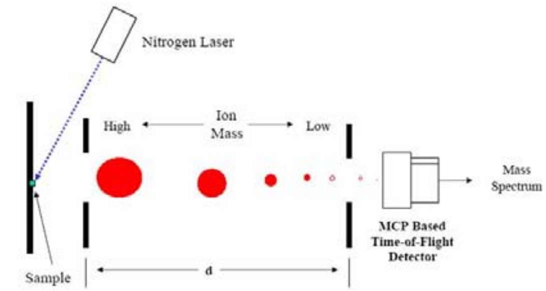

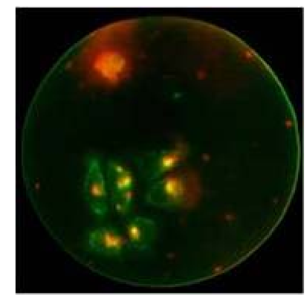

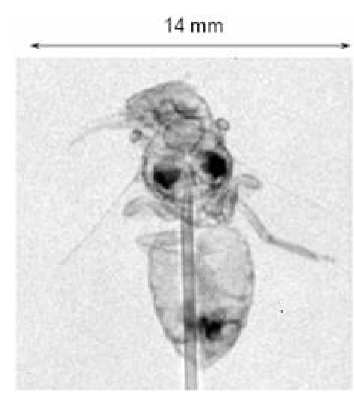

MCP detector configuration

- Photocathode converts photon to electron
- MCP(s) amplify electron by 10^3 to 10^7
- Rear field accelerates electrons to r
- Different readou used, optimiz particular application

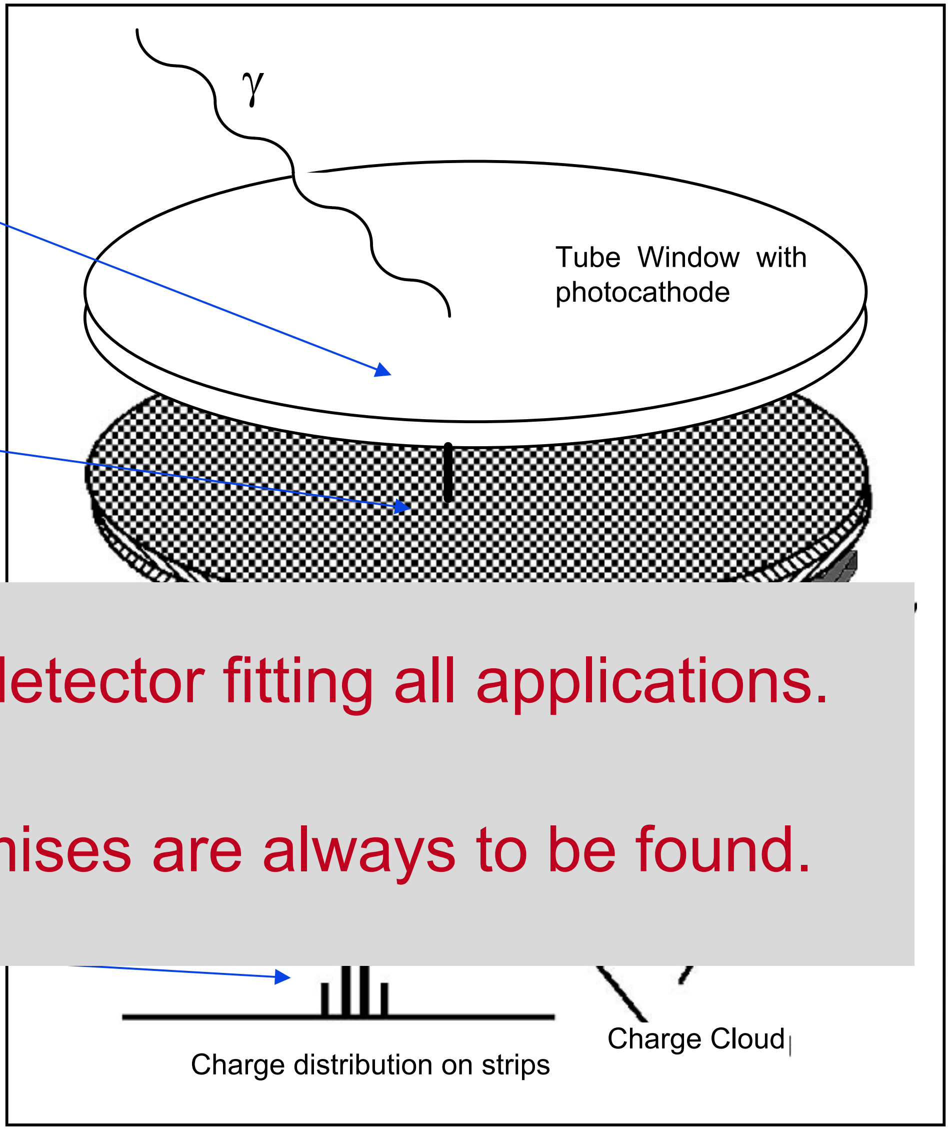

No ideal detector fitting all applications.

Compromises are always to be found.

MCP detectors vs conventional imaging devices

MCP detectors	Frame-based devices (CCD, image intensifiers)
• **No readout noise**	• **Reconfigurable active area**
• **High detection efficiency (neutrons, soft X-rays)**	• **No high voltage**
• **Time and position for every detected particle** (~10-30 µm and ~10-100 ps, photons, electrons, ions, alphas; <0.5 µs thermal, ~10 ns epithermas neutrons)	• **No vacuum**
• **Event counting**	• **Commercially available sensors,** well established technology
• **TOF applications**	• **Easy to operate**
• **High counting rates** possible with latest readouts (~1 GHz no timing resolution, >20 MHz with timing resolution)	• **Very uniform response in active area**
• **Small area**	• **Readout/dark noise**
• Require **vacuum**	• **Stroboscopic mode in TOF experiments**
• Require **high voltage**	• Limited **time resolution**
• **Image distortions**	• **Cooling required**

Highly generalized

Detector hardware implementations

Synchrotron beamline detectors:
ARPES – angular resolved
photoelectron emission spectroscopy

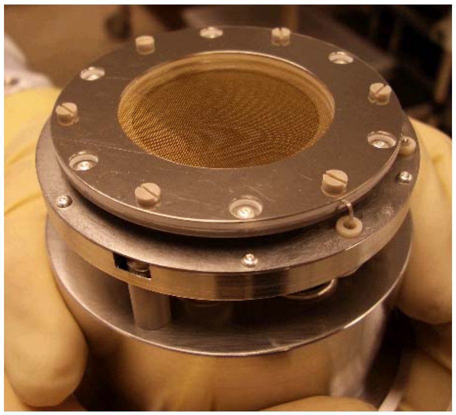

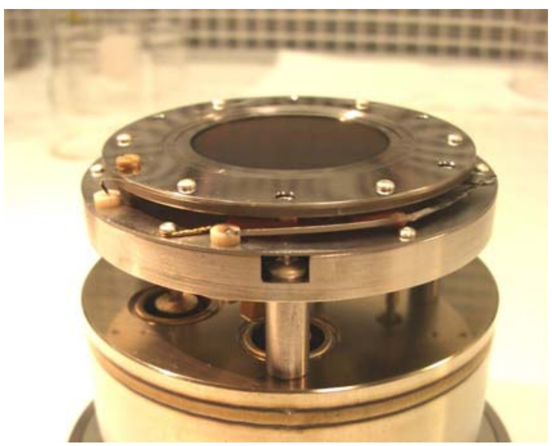

COS detector
Installed on Hubble telescope

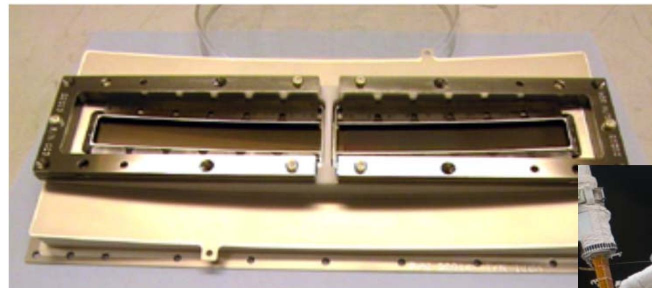

NASA Shuttle STS-125 Mission

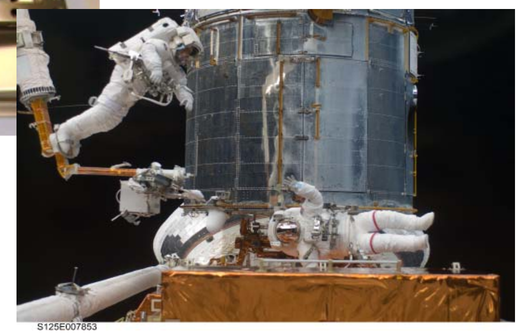

Sealed tube configuration
(Galex NASA mission)

Neutron imaging
device

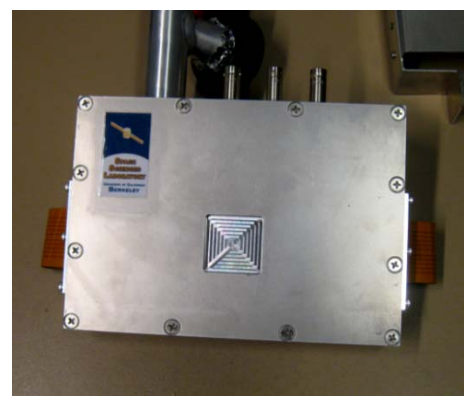

Detectors developed at SSL for NASA applications

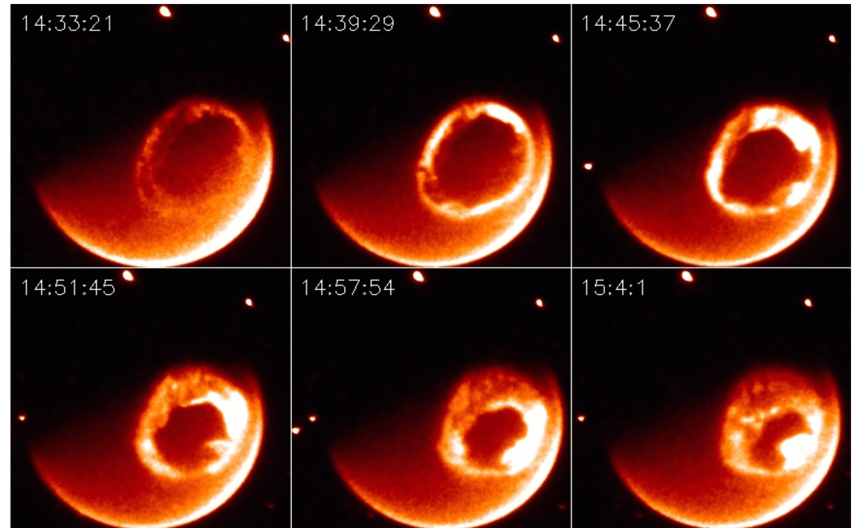

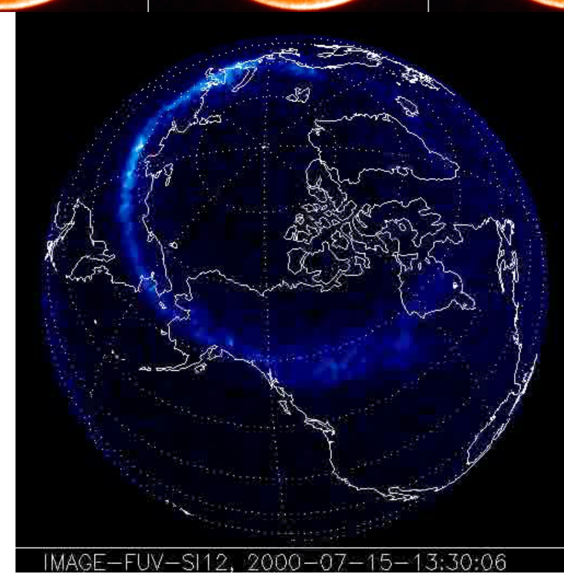

S. Mende, et al., Space Science Reviews, **91** (2000), pp.271-285.

Bioimaging applications (FRET, FLIM, etc)

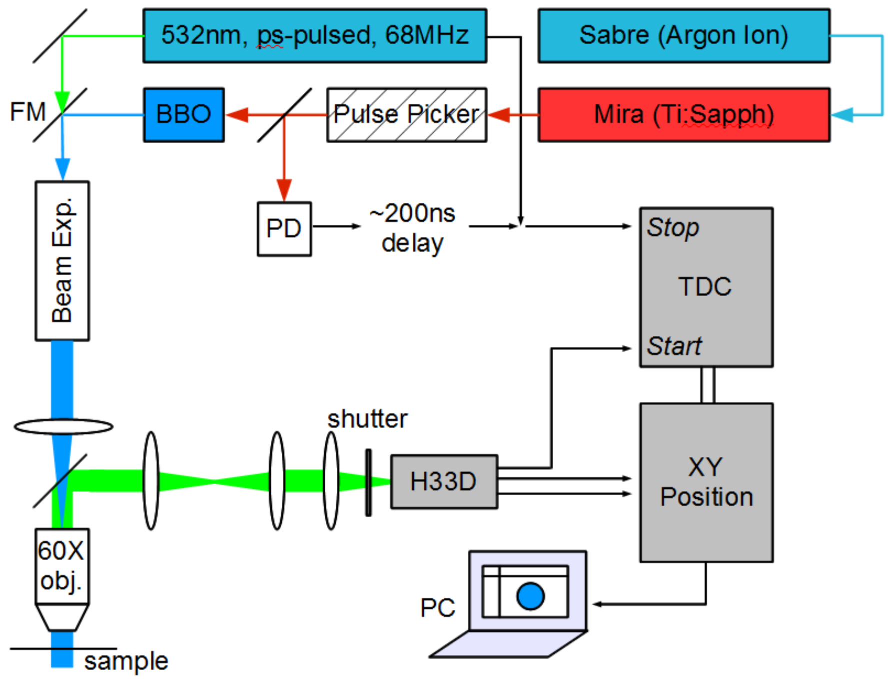

X. Michalet, R.A. Colyer et al., UCLA, Current Pharmaceutical Biotechnology10(5), pp. 543-558 (2009).

Bioimaging applications (FRET, FLIM, etc)

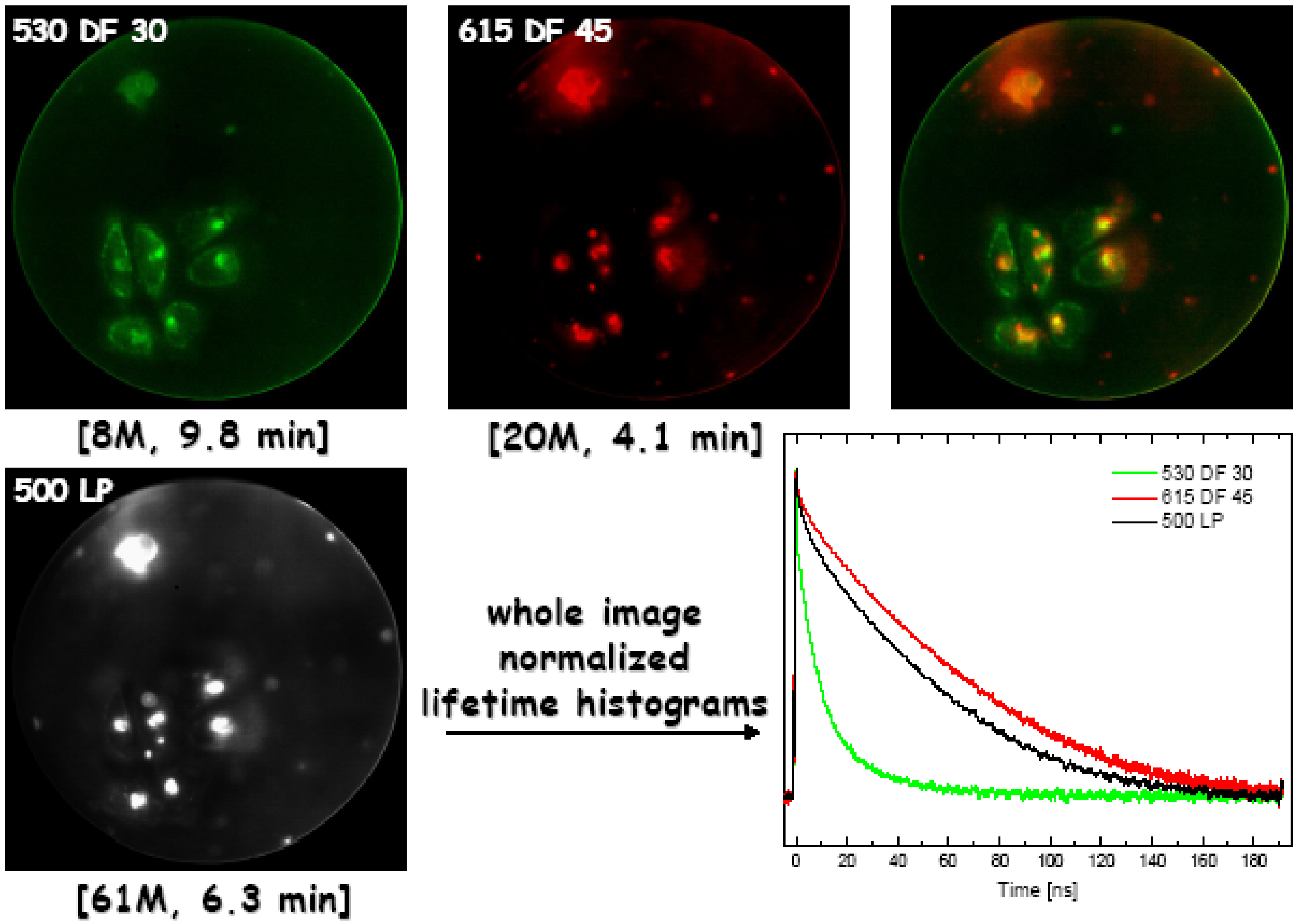

X. Michalet, R.A. Colyer et al., UCLA, Current Pharmaceutical Biotechnology10(5), pp. 543-558 (2009).

Readout types

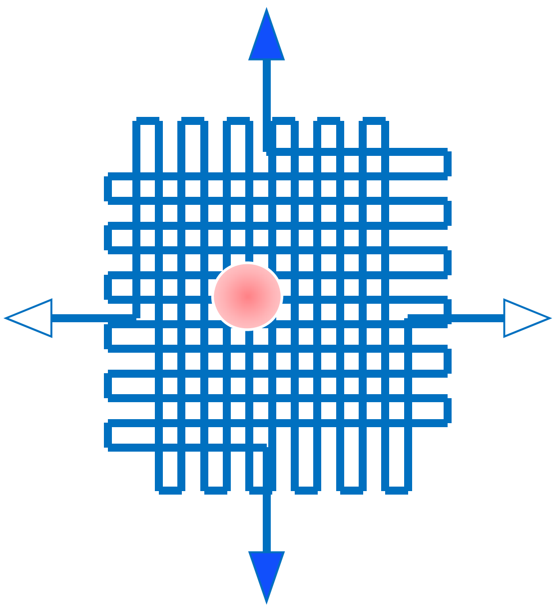

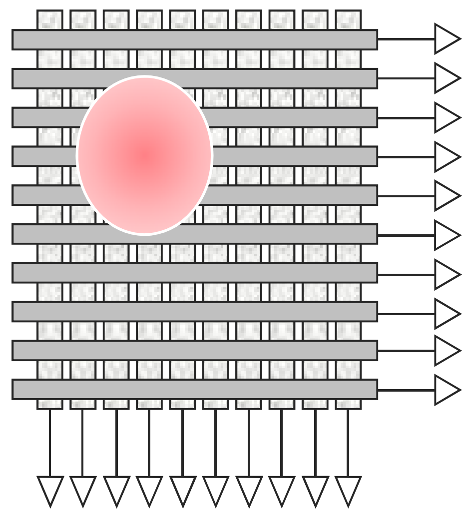

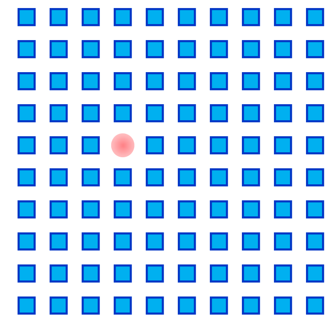

Cross Delayline (XDL)	Cross Strip (XS)	Medipix/Timepix ASIC
4 amps	2 x N amps	N x N amps
Gain ~ 10^7	Gain ~ 10^6	Gain ~ 10^4-10^5
Rate < 1MHz	Rate < 5MHz	Rate > 200MHz
Δt ~ 50 ps rms	Δt ~ 100 ps rms	Δt ~ 10 ns - 1 ms

Spatial resolution of MCP detectors

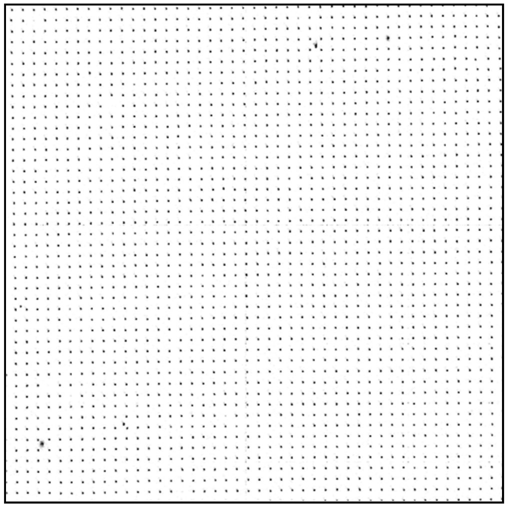

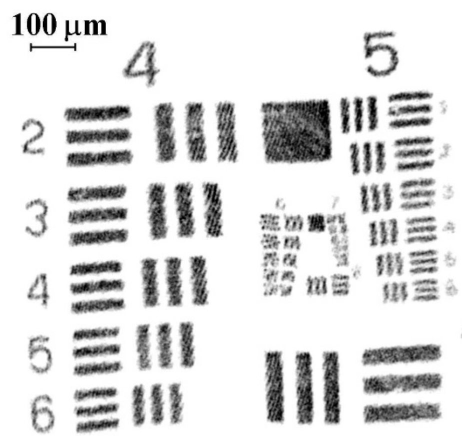

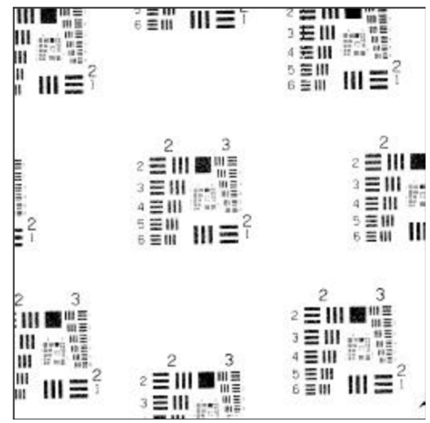

•XDL readout

•Very linear images

•Resolution ~20μm FWHM and 50 ps rms

•Large Formats (20cm x 20cm)

•Gain ~10^7

•Global event rates <1 MHz

•XS readout

•Very high resolution ~10 μm FWHM and ~100 ps rms

•Gain ~10^6

•Event rates < 5 MHz

•CMOS readout

•Resolution ~55μm FWHM and ~10 μm FWHM with event centroiding

•Very high event rates >1 GHz (no centroiding, no timing)

•Gain <10^5

•Small active area 28x28 mm^2

Timing resolution of XDL detectors

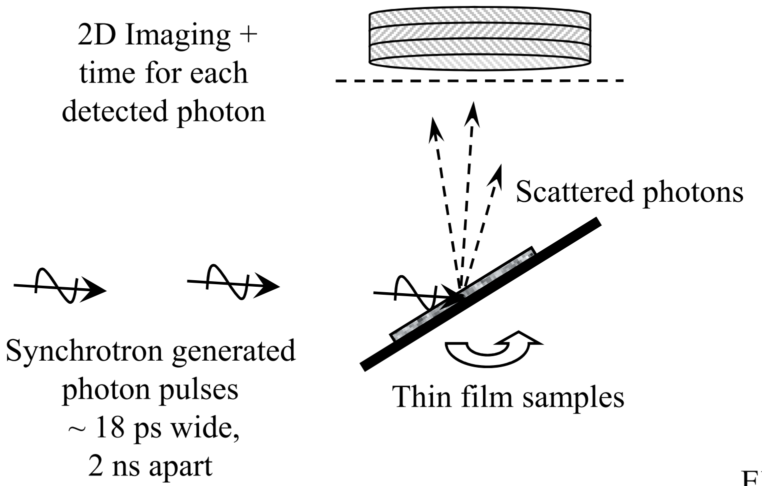

Elastically scattered photons

Timing accuracy 55 ps RMS
(130 ps FWHM)

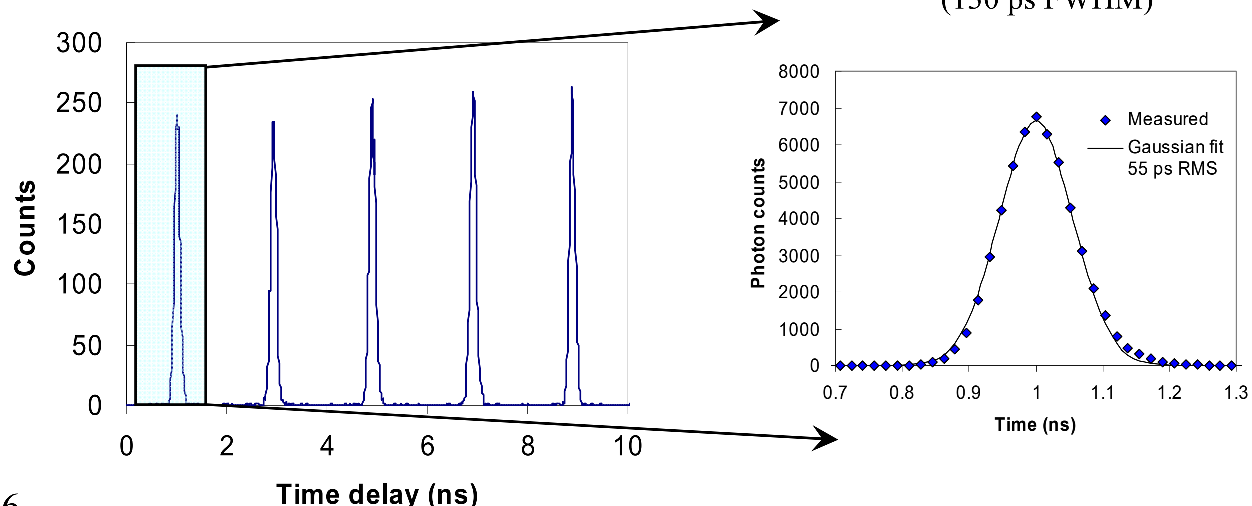

IEEE Trans. Nucl .Sci. 54 (2007) 706

Synchrotron bunch diffusion

Bunch population after injection

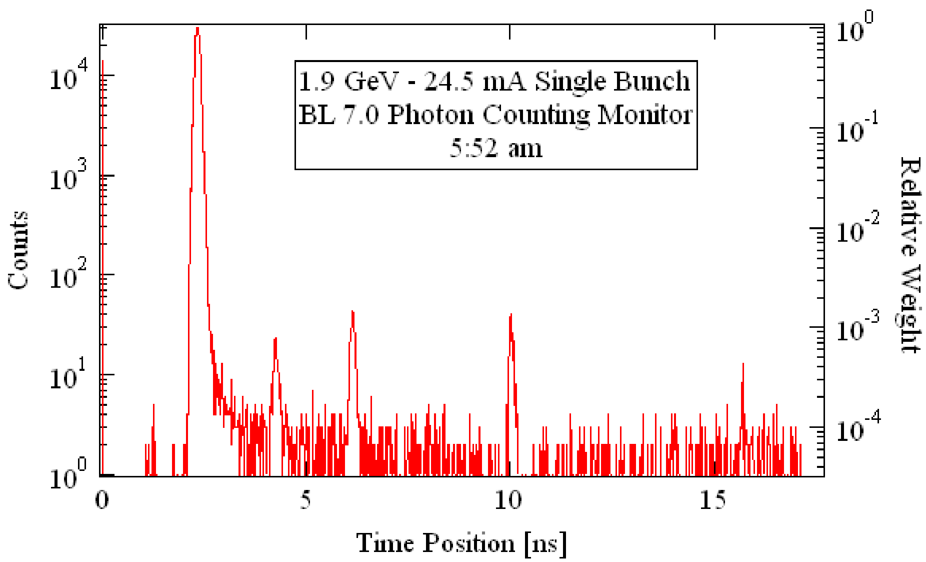

Bunch population ~76 min later

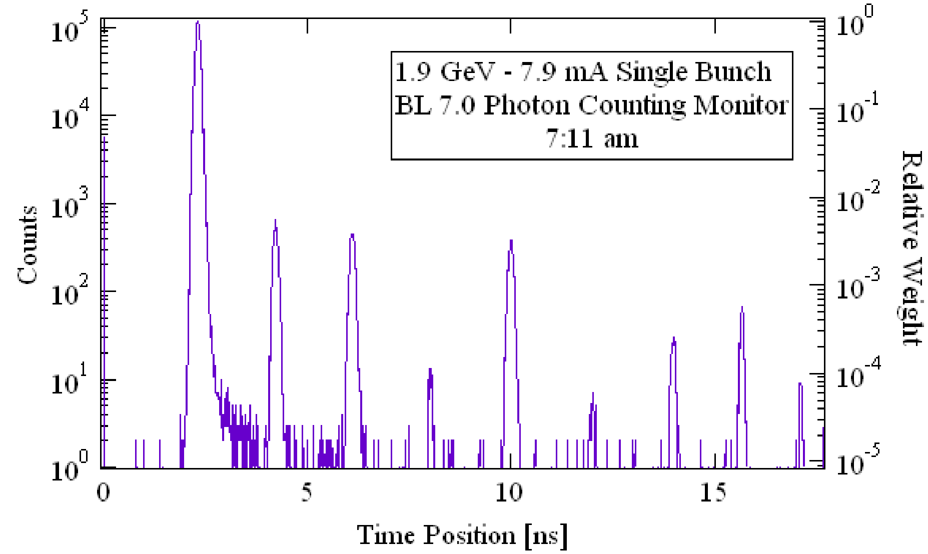

Diffusion of electrons between the adjacent bunches was optimized with MCP detection system

W. E. Byrne, C.-W. Chiu, J. Guo, F. Sannibale, J.S. Hull, O.H.W. Siegmund, A. S. Tremsin , J.V. Vallerga
Proceedings EPAC'06, Edinburgh, June 2006

Delay line readout

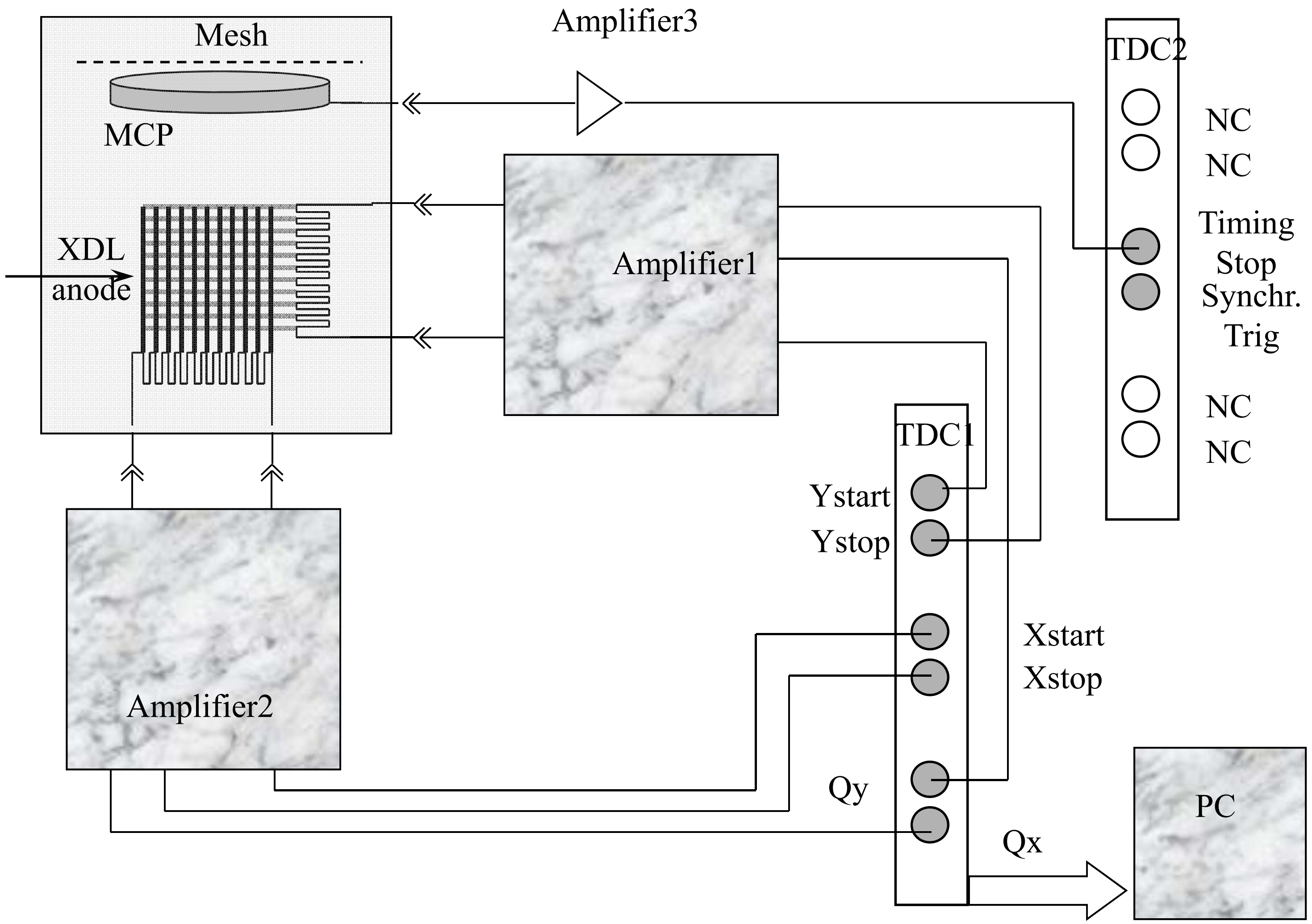

Cross strip readout

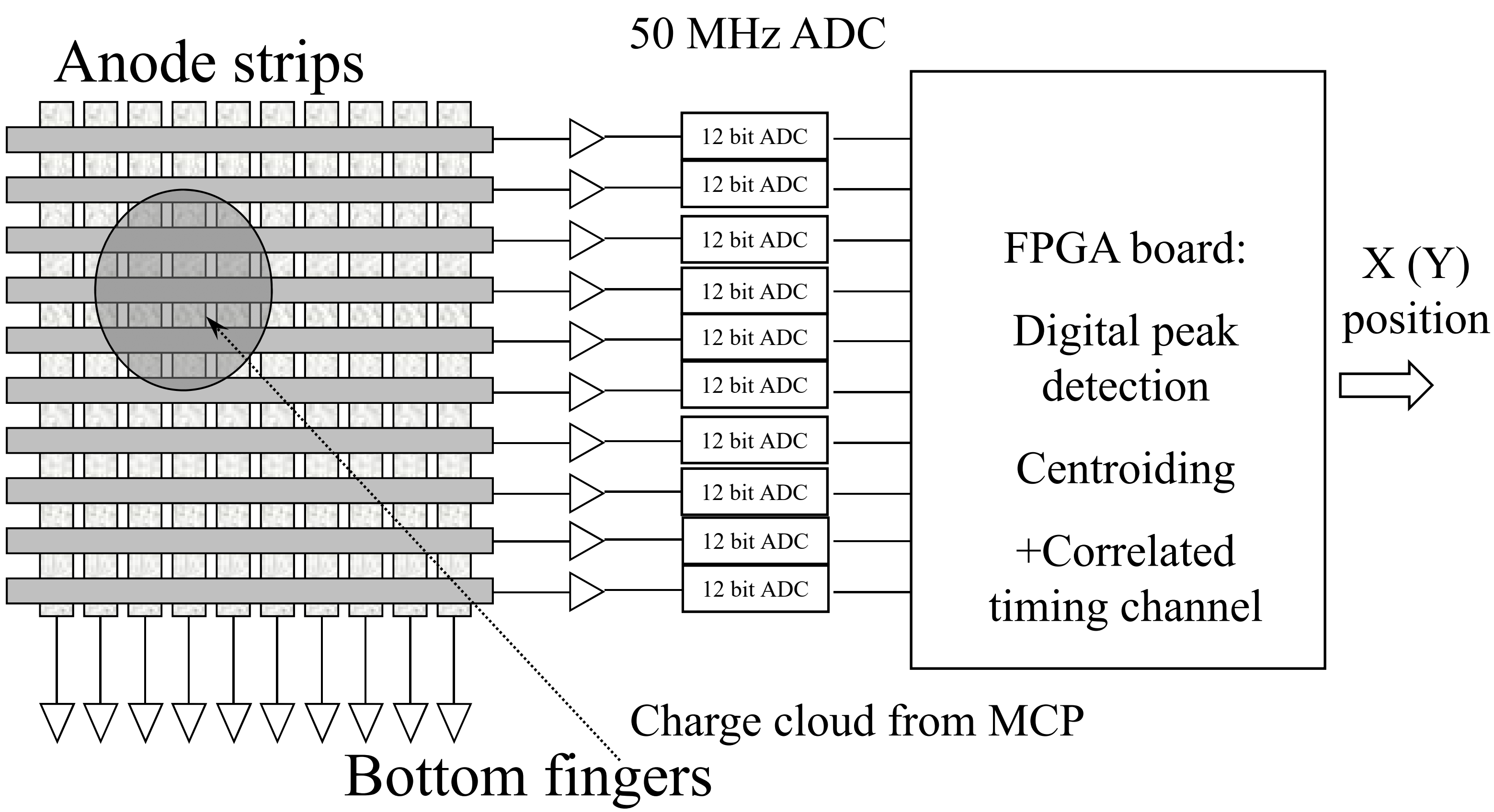

Each finger has its preamplifier followed by an ADC, continuously digitizing the signal.

Centroiding done on digitally calculated charge values.

O. Siegmund, et al., Nucl. Instr. and Meth. A 610, pp.118-122 (2009)

32x32 mm^2 XS

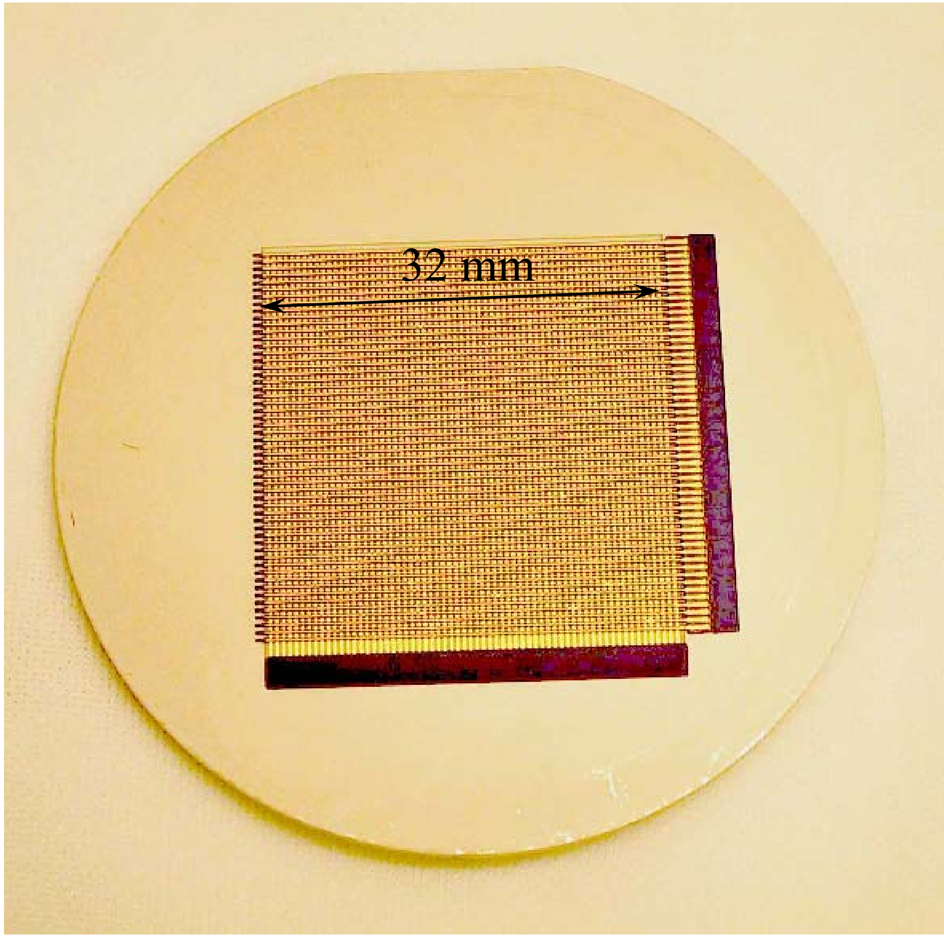

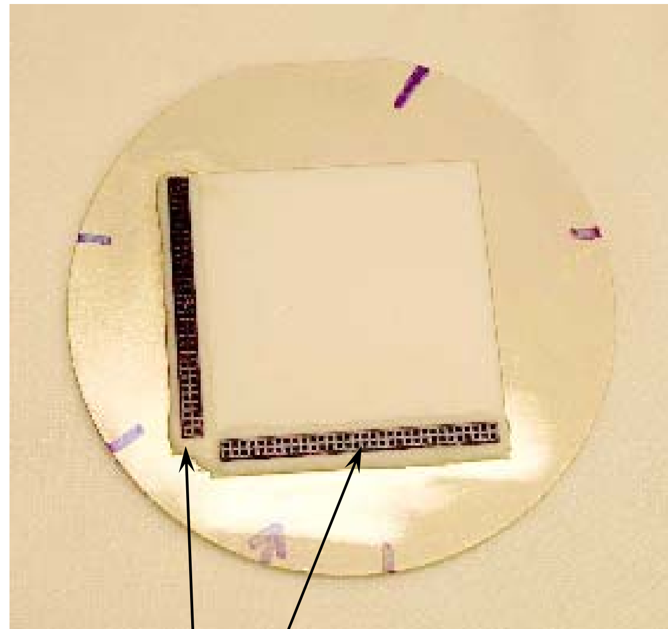

•32 mm long electrodes on 0.5 mm period

•Hermetically sealed holes

Back end connectors for ASIC mounting

XS anode spatial resolution

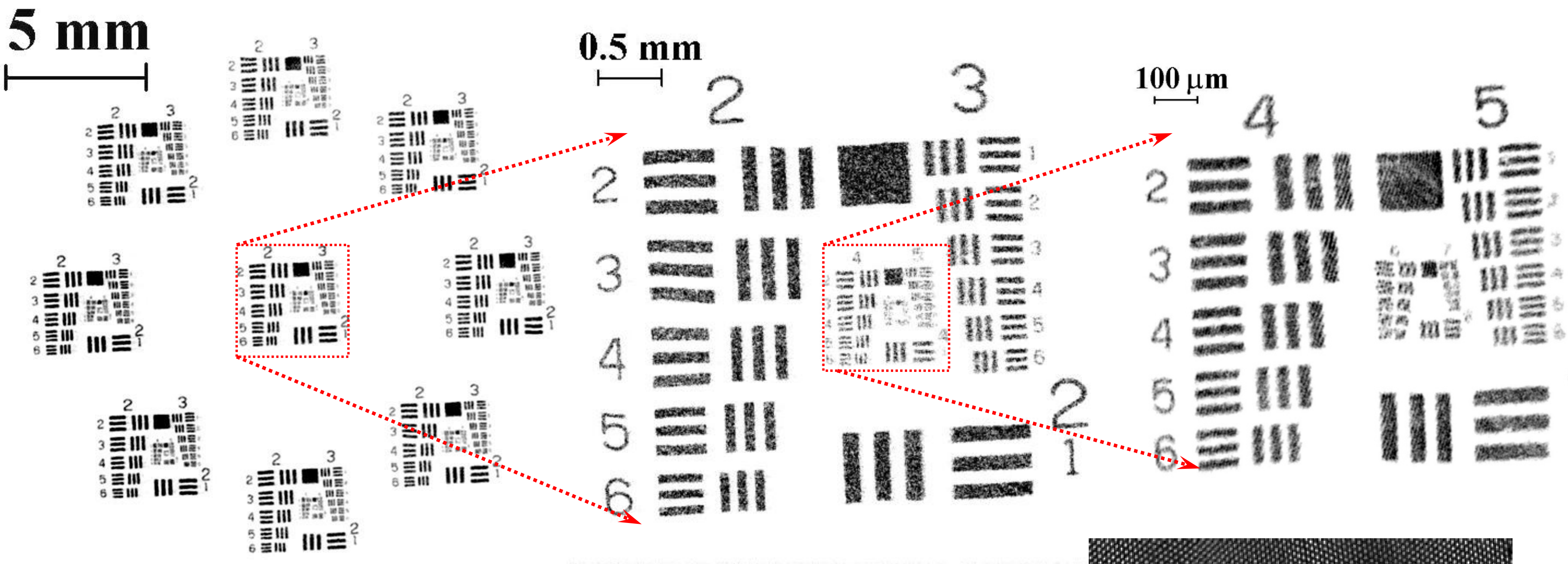

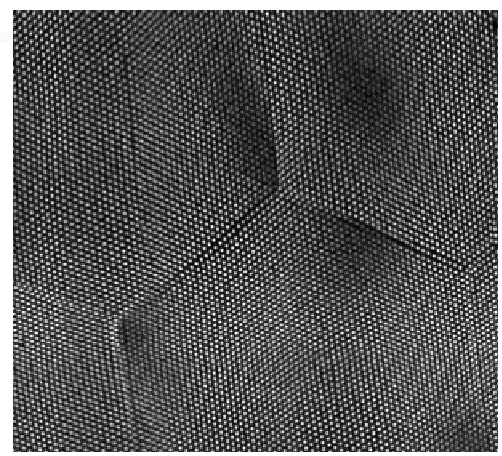

12 μm MCP full filed illumination image

18mm Cross Strip Sealed Tube with SuperGenII Photocathode

22mm round cross strip anode used in sealed tubes has a 0.7mm period. Through hole vias transfer the charge to the back of the anode and a fanout permits connection to a standard connector. SuperGen-II cathode on glass window.

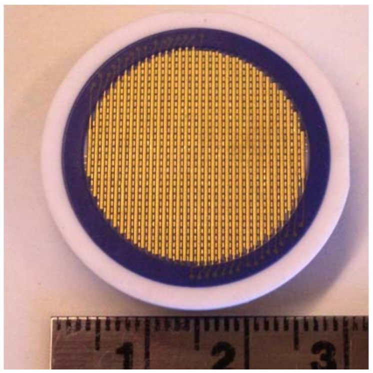

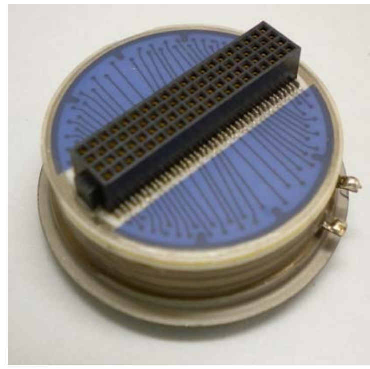

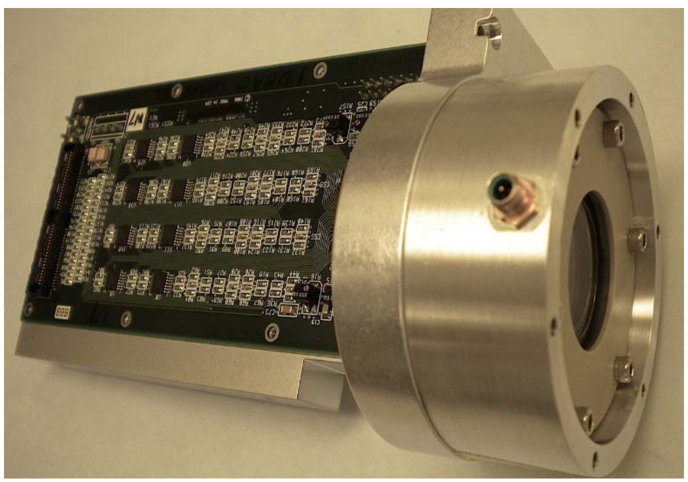

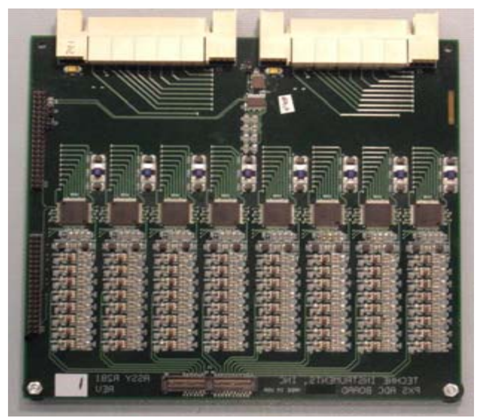

Parallel 64 channel ADC

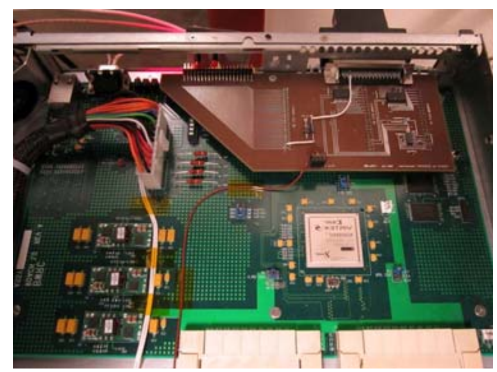

Virtex 5 FPGA board

18mm Cross Strip Sealed Tube with SuperGenII Photocathode

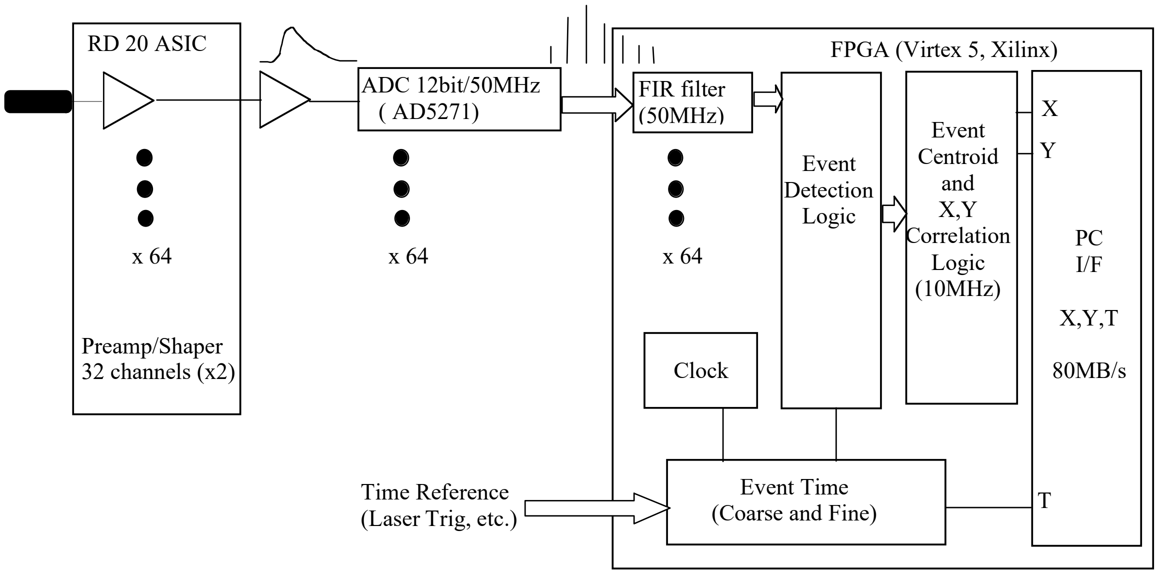

Schematic of PXS electronics including Preshape32 amplifiers, ADCs and Virtex FPGA.

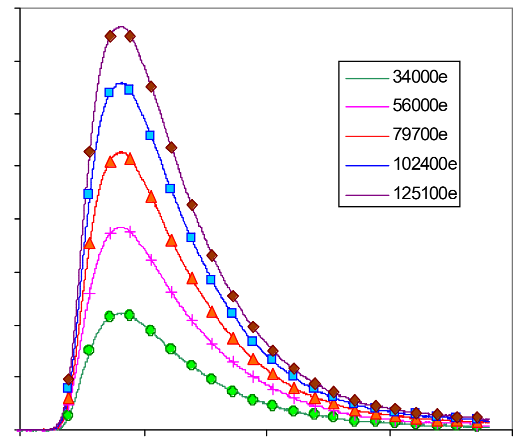

Example of signal shapes for various charge pulses from the Preshape32 ASIC sampled by the PXS box at 60 MHz (16ns steps) showing the ~45 ns risetime and the ~200 ns fall time.

J.V. Vallerga at al., Proc. of SPIE Vol. 7732 773203-3
J.V. Vallerga, et al., Astr. Telescopes Instr. SPIE 2016

MCP detector with Medipix/Timepix readout

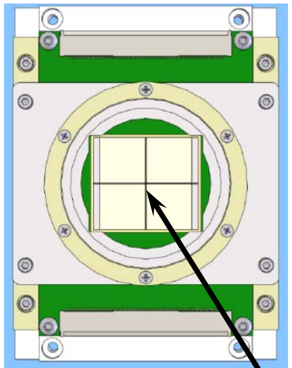

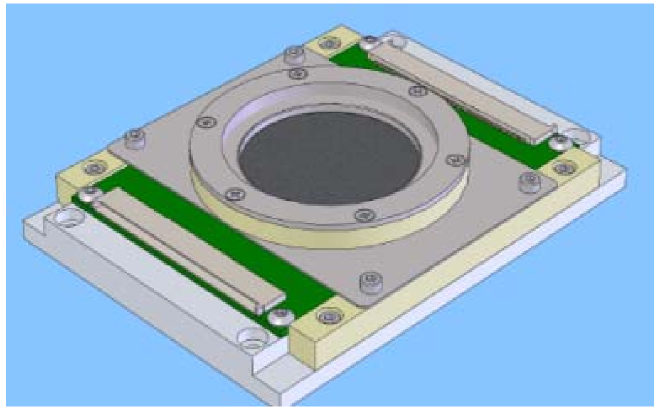

Stack of MCPs is positioned 0.5 mm above Timepix readout.

2 x 2 array of Timepix ASICs

The assembly is placed in vacuum container

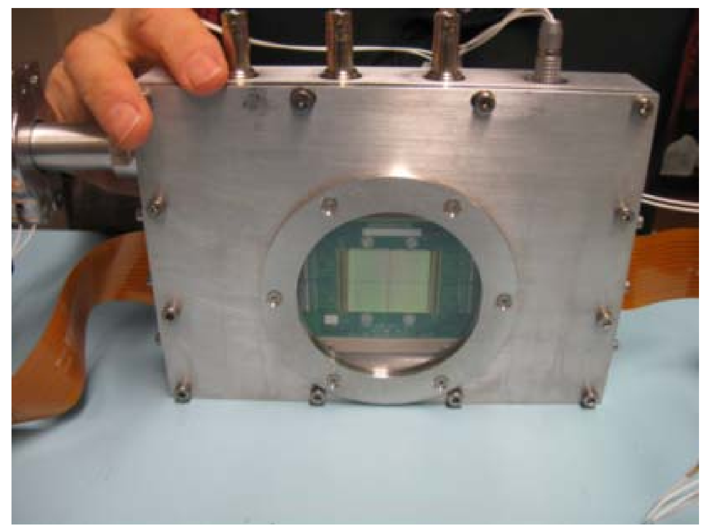

- 512 x 512 array of 55 μm pixels (28x28 mm^2 area)
- 100 kHz/pixel
- Frame rate: >1 kHz
- Low noise (<100e^-) = low gain operation (10 ke^-)
- ~1 W watt/chip, 3-sides abuttable
- ASIC developed at CERN for Medipix collaboration

MCP detector with Medipix/Timepix readout

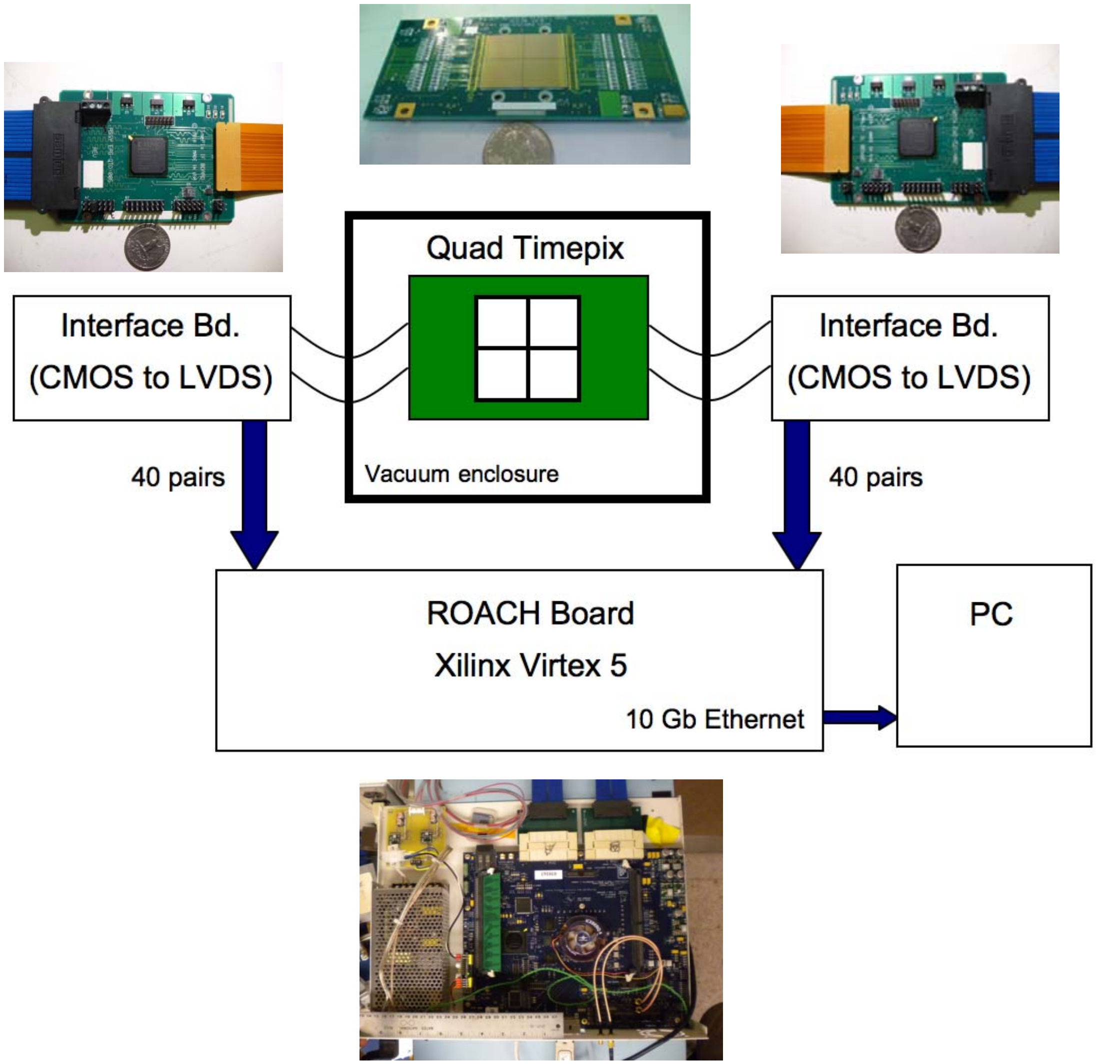

- Up to 1200 frames/sec
- Readout time ~283 μs
- 3 acquisition modes.
  Each pixel provides either:
  - Event counts (image integrated on the chip)
  - Time of event (up to 10 ns accuracy)
  - Charge accumulated in a pixel (ToT mode)

Timepix readout for MCP detectors

- Simultaneous events can be detected (up to ~25000).
- The same detector: event counting or frame-based imaging.
- Operate at low gains (10^4-10^5).
- Can operate at very high counting rates exceeding 100 MHz/cm^2 (55 μm resolution) or at rates of ~2-3 MHz per 2x2 Timepix readout with resolution of <10 μm.
- Analog amplification in pixels, only digital signals read out.
- No readout noise
- Very uniform readout (lithographic processing) – no image distortions.

3 modes of event counting/imaging

1. **Event counting in each pixel**
   - up to 11800 events per pixel/frame
   - ~10 kHz rate/pix
   - detector global rate >100 MHz with no resolution degradation
   - local counting rate ~100 kHz
   - spatial resolution = 55 μm pixel
   - time resolution = shutter length (1μs-seconds)
   - can be synchronized to external trigger (stroboscopic imaging)

2. **Time of event : internal clock or relative to external trigger**
   - 1 event per pixel/frame (~25K events/frame)
   - time bin from 10 ns
   - time range = 11800 x time bin
   - spatial resolution = 55 μm pixel
   - multiple shutters per trigger

3. **Charge in pixel**
   - 1 event per pixel/frame (~25K events/frame)
   - spatial resolution = 55 μm pixel
   - time resolution = shutter length (1 μs to secondss)
   - can be synchronized to external trigger
   - multiple shutters per external trigger

MCP/Timepix sealed tube detector (produced by Photonis)

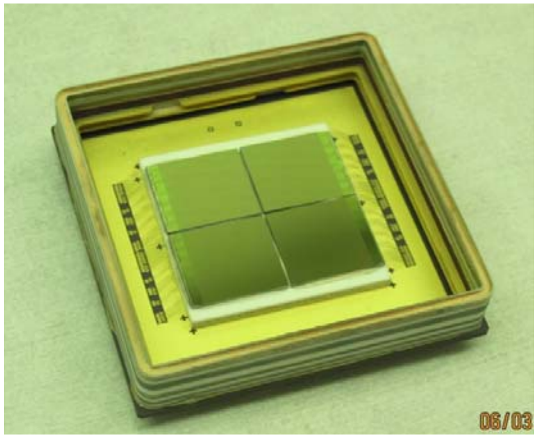

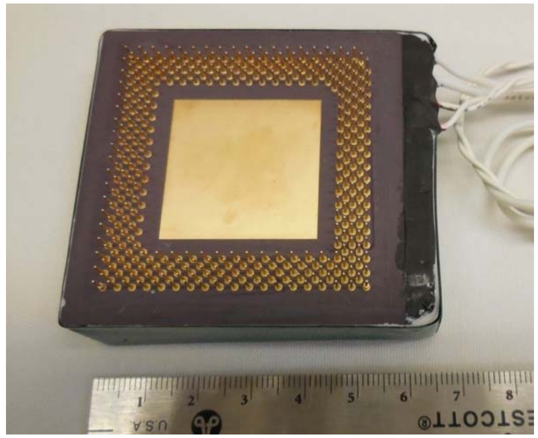

Pulsed diode (~100 ns)

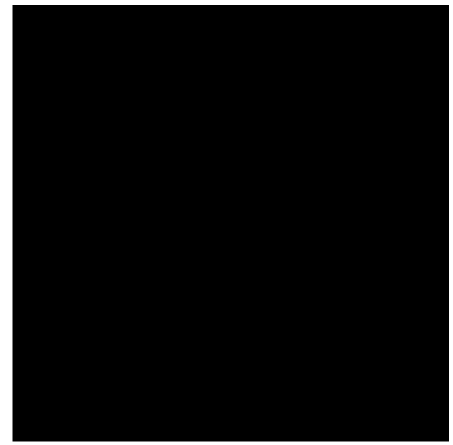

PI J.V. Vallerga

Individual photons

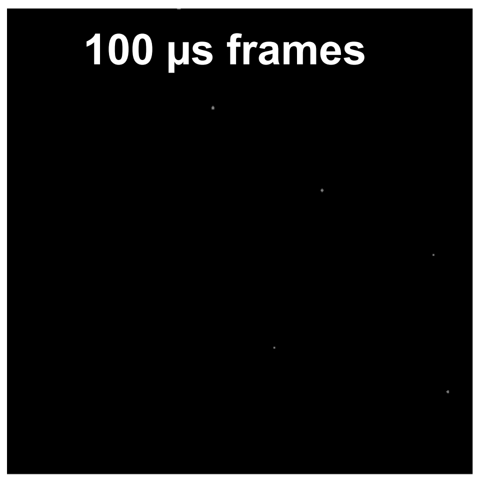

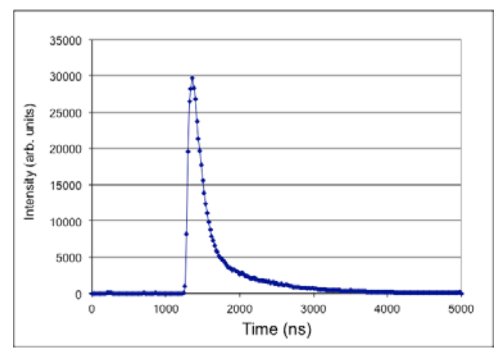

J.V. Vallerga, et al., Journal of Instrumentation JINST 9 C05055 (2014).

MCP/Timepix sealed tube detector (produced by Photonis)

Photo:Bay Bridge at night

Phase imaging from individual photons

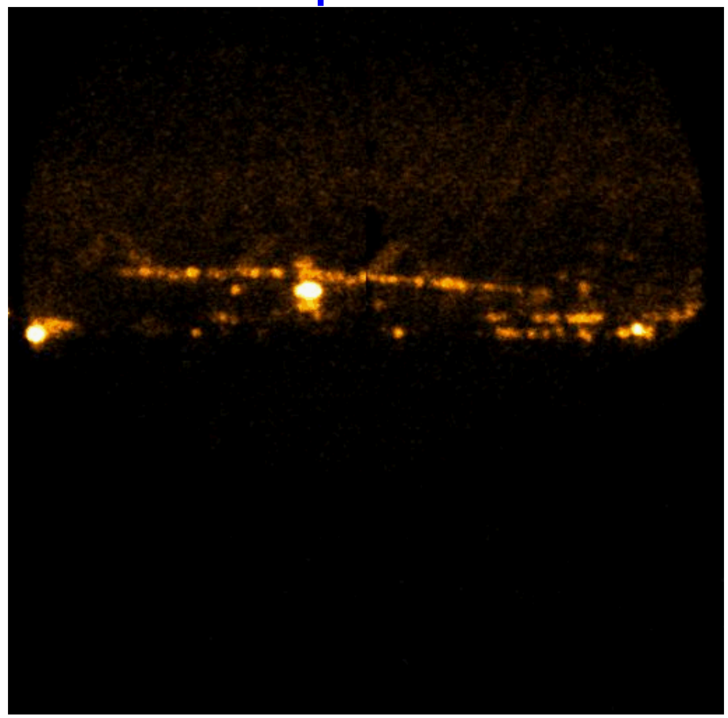

Individual phases

Phase 1

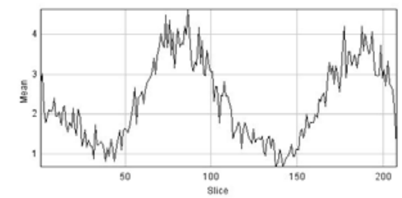

Phase 2

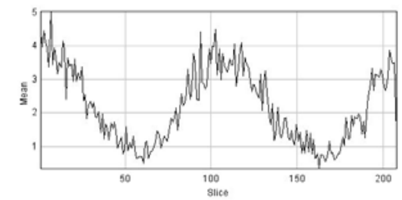

Phase 3

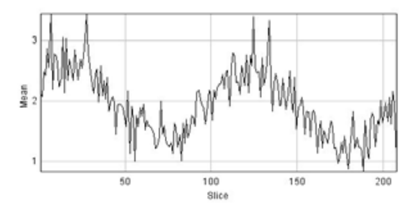

Photons timed and phased to a single period of 60Hz line frequency. Lightcurves of 3 different pixels shown at right.

PI J.V. Vallerga

J.V. Vallerga, et al., Journal of Instrumentation JINST 9 C05055 (2014).

Mode 1: Frame-based / event counting mode

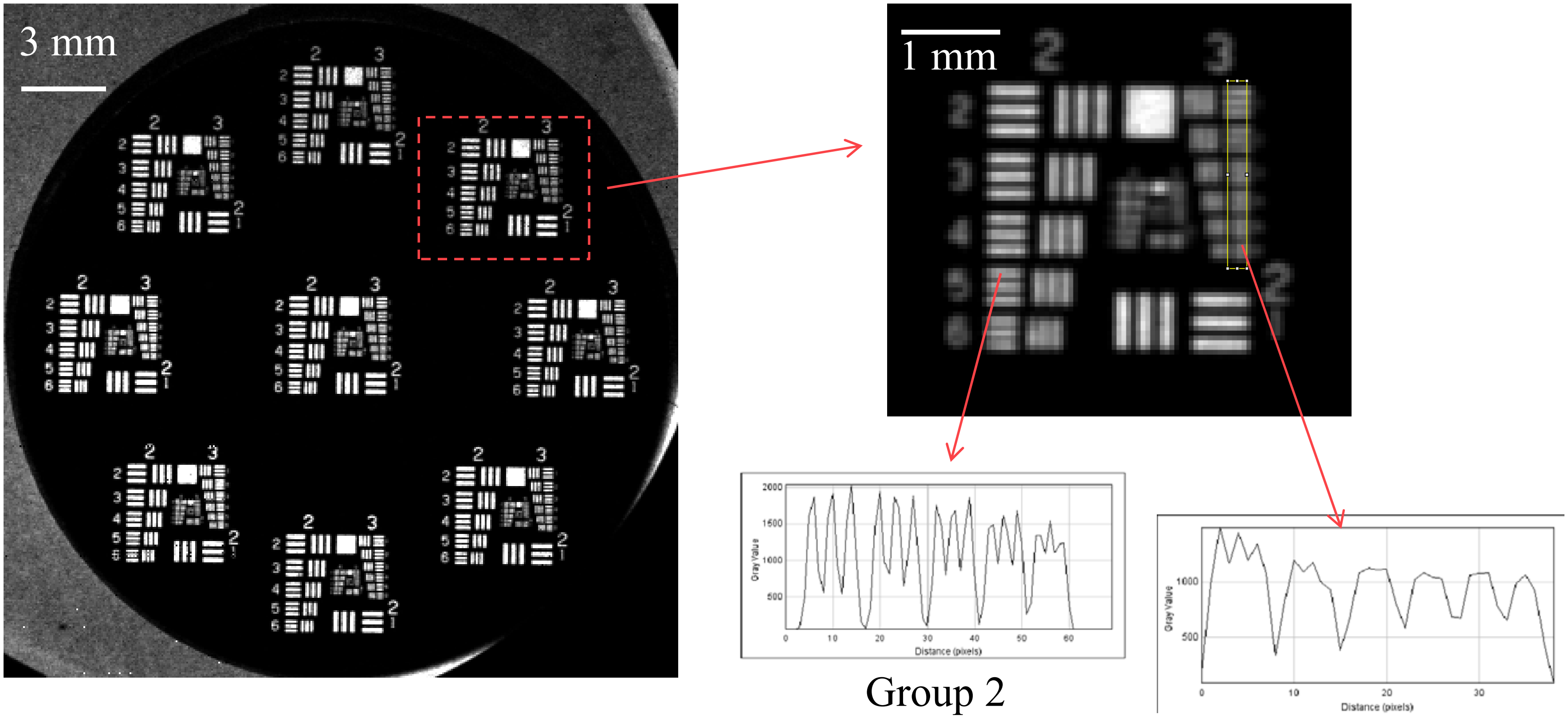

Group 2

Group 3

High count rates are possible.
Up to 11800 counts per pixel before readout out.

Resolution limited by ~55 μm pixels

Mode 2: Time of each event

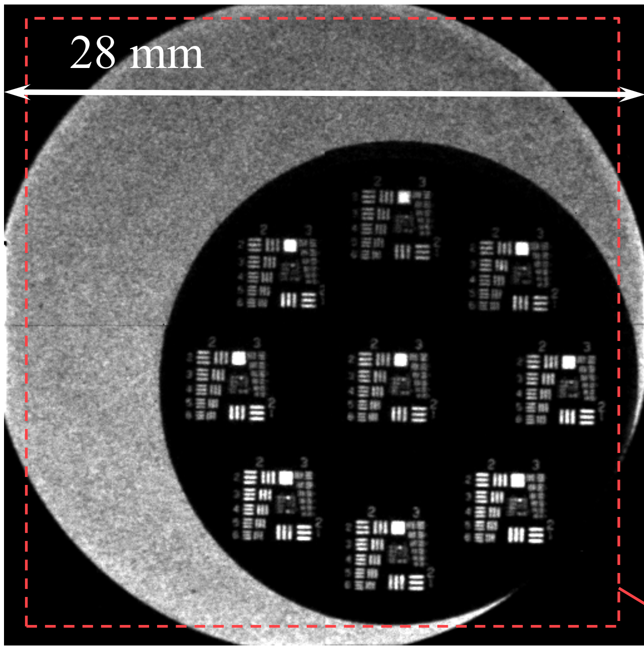

UV penray lamp intensity fluctuations (60 Hz AC)

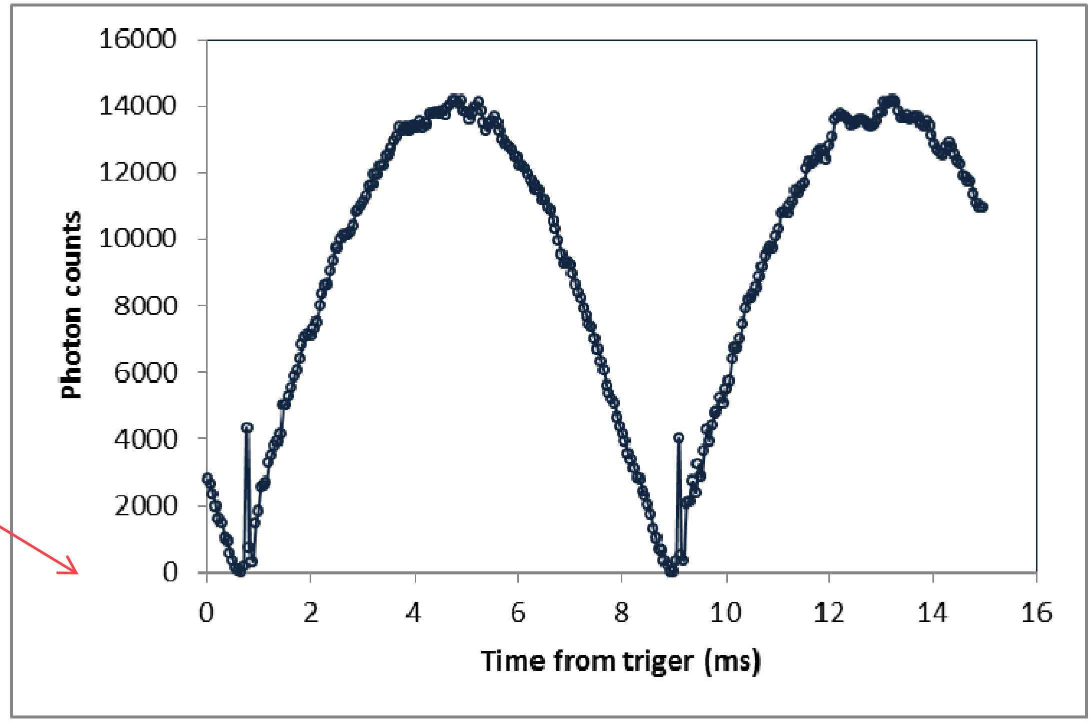

Timing of each event relative to external trigger is measured.

Time histogram is accumulated in each pixel.

Resolution limited by ~55 μm pixels

Mode 3: Event centroiding

High resolution imaging with resolution ~ MCP pore is possible

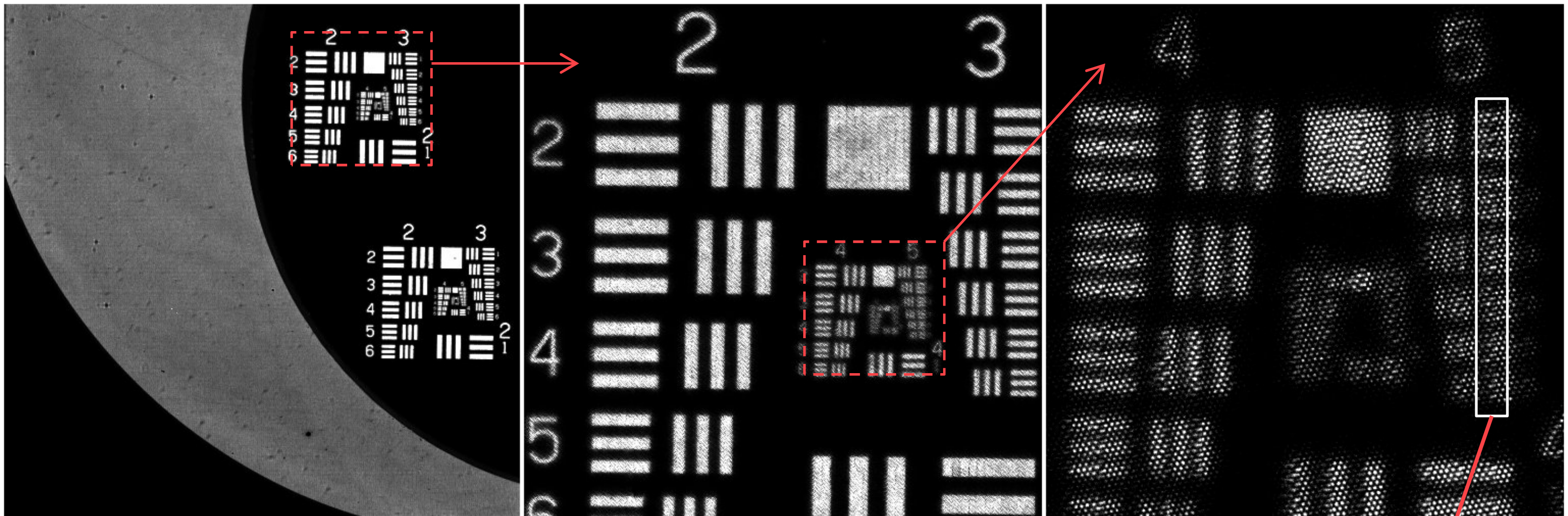

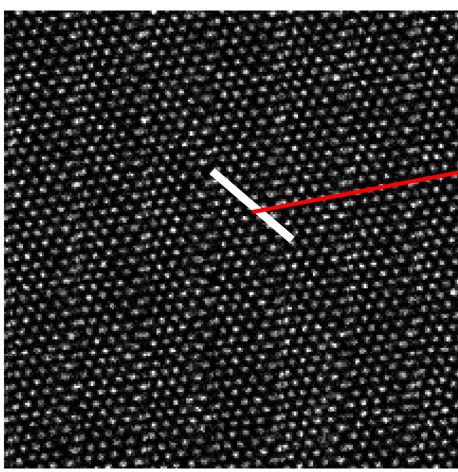

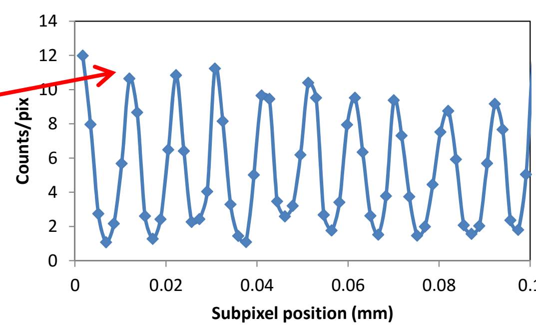

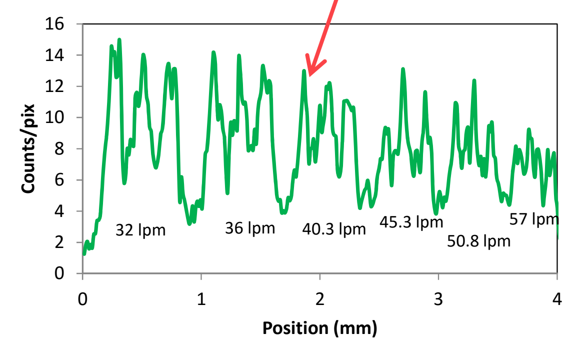

Readout resolution ~4 µm FWHM

Nucl, Instr. Meth. A 787 (2015) pp. 20-25.

An ideal photocathode

- High quantum efficiency
- Stable in time, stable under air exposure
- Radiation hard
- Fast
- Solar blind
- No thermionic electron emission
- Easy to manufacture
- Do not require operation in high vacuum
- Can be deposited on different substrates
- …

Does not exist ⇒ To be optimized for a particular application

Hamamatsu image intensifiers

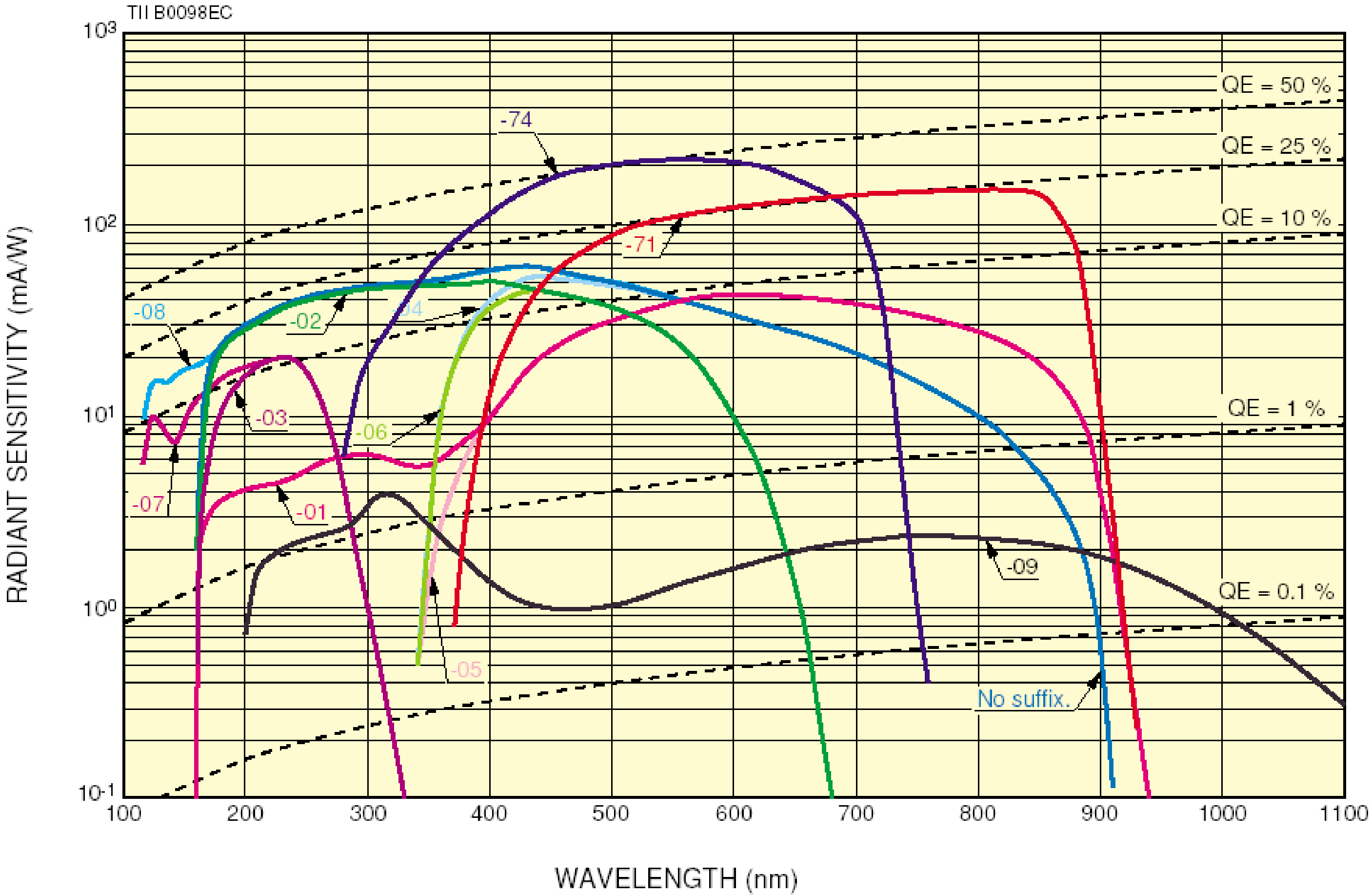

01 – Extended red multialkali
03 - CsTe
71 - GaAs
74 – GaAsP

Photocathode Efficiency

- Photon absorption length (μ)
- Photoelectron escape length ($\mathbf{L_s}$)
- Photoelectron escape probability (**P**)
  (surface work function or electron affinity)

Photocathodes deposited on the window at high temperatures. Window is transferred to the processing chamber.

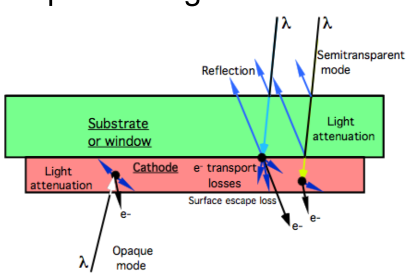

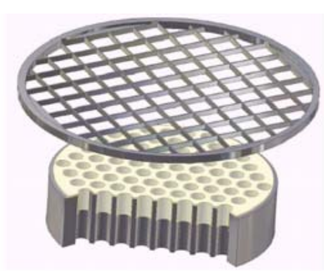

Photocathodes deposited directly on MCP
Electron repelling mesh

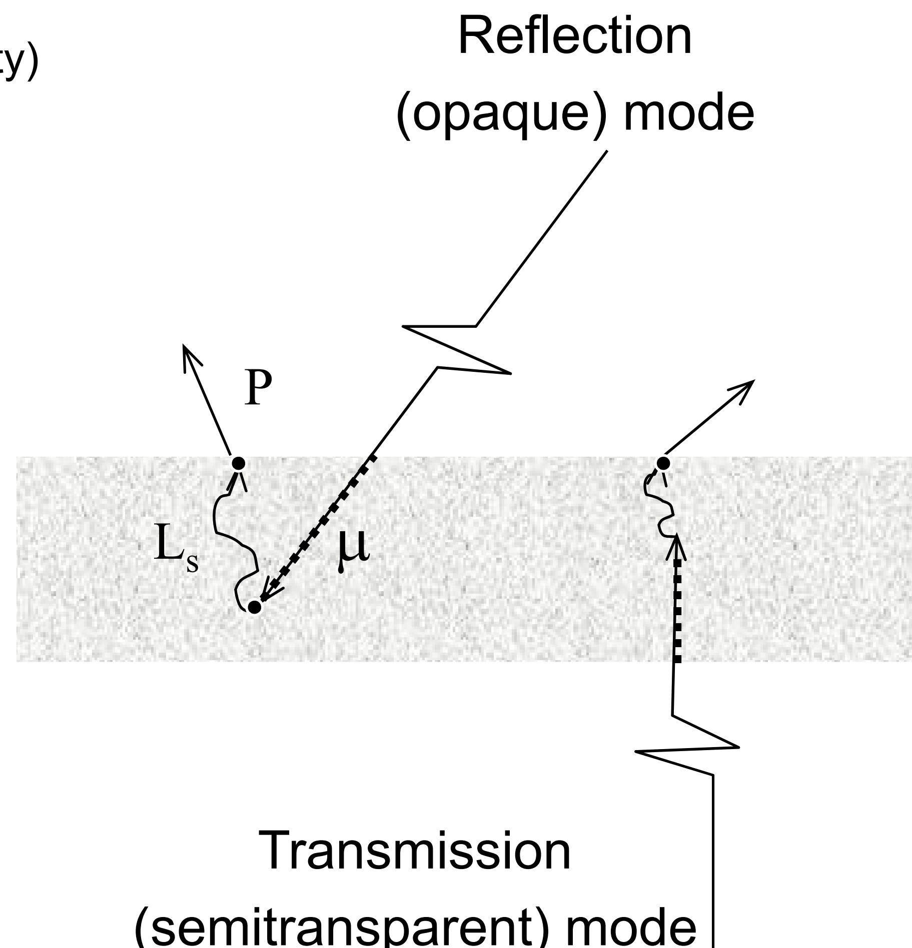

UV and soft X-ray photocathodes

Quantum Efficiency of alkali halide photocathodes

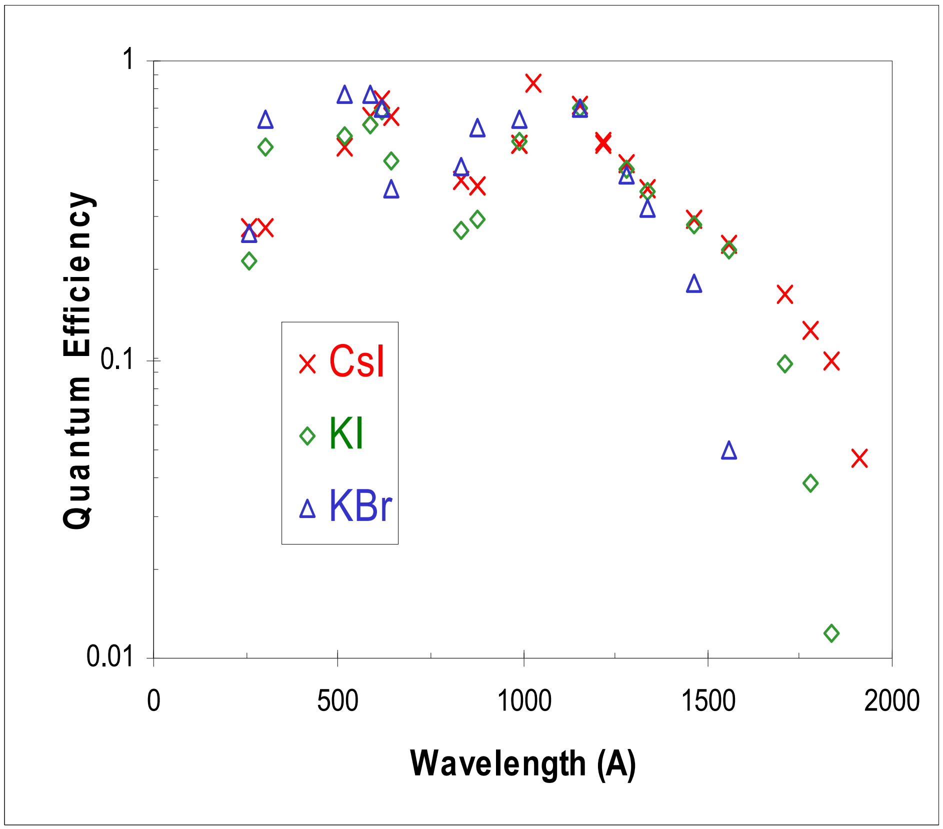

Reflective

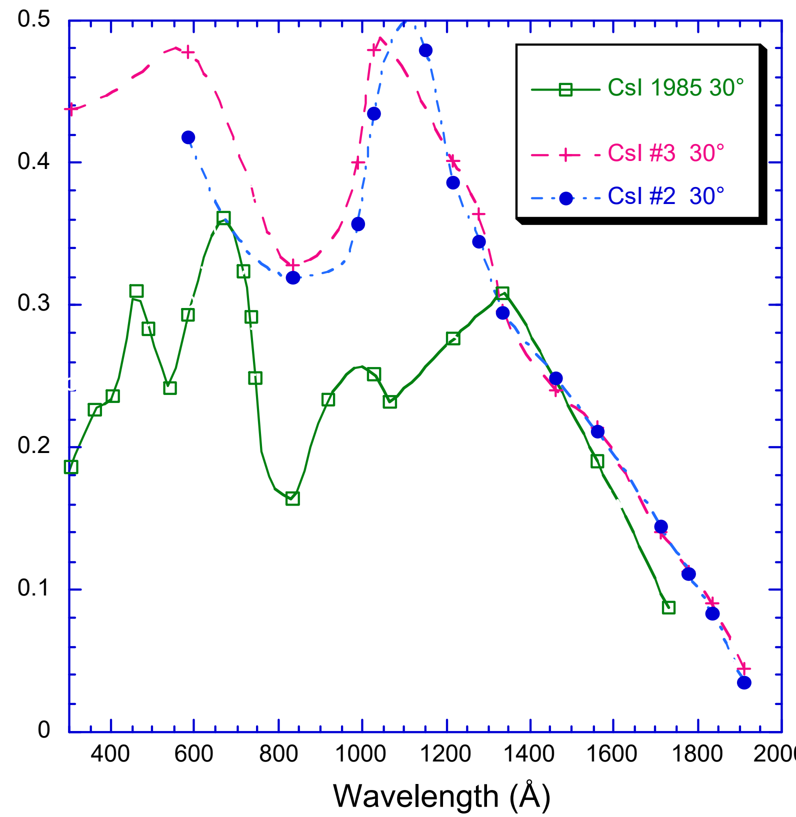

Opaque on MCP

UV and soft X-ray photocathodes

Quantum Efficiency of alkali halide photocathodes

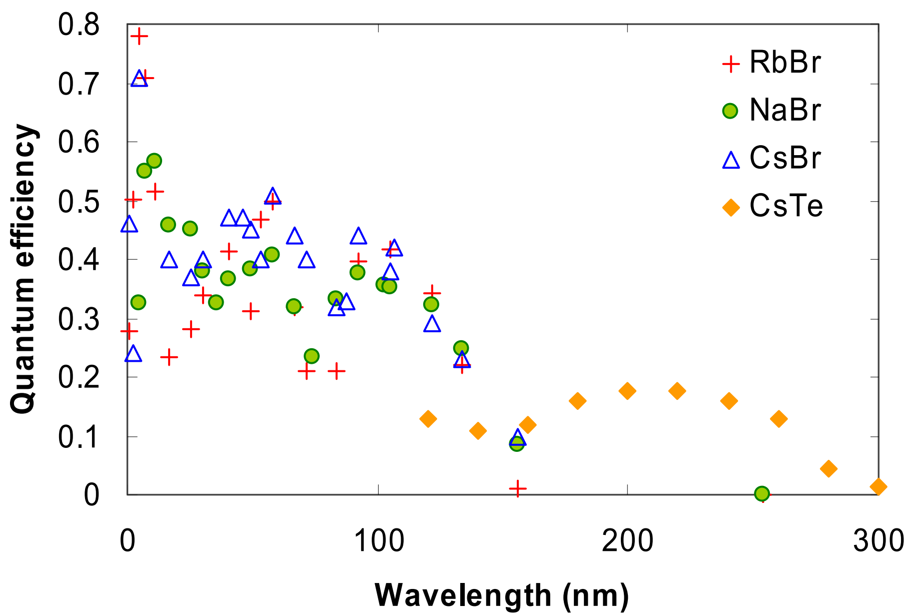

As function of wavelength

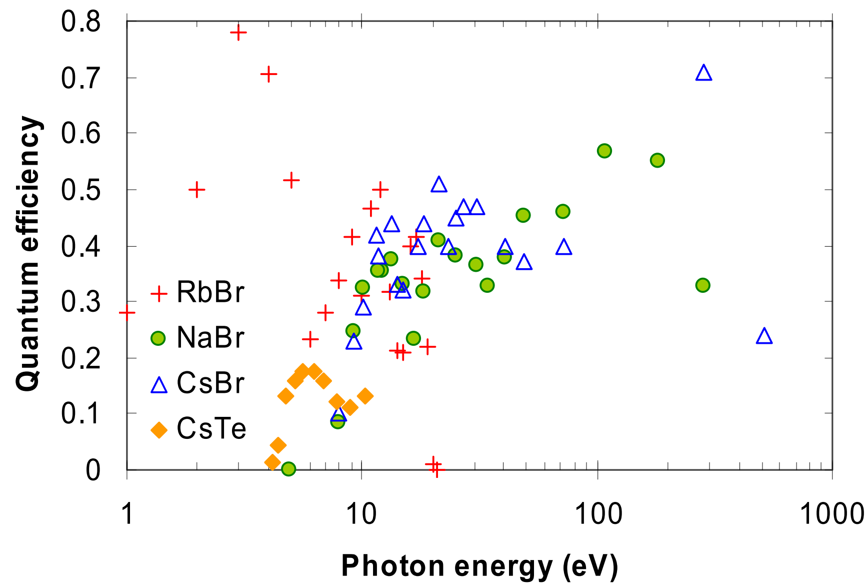

As function of photon energy

UV and soft X-ray photocathodes

Quantum Efficiency of alkali halide photocathodes

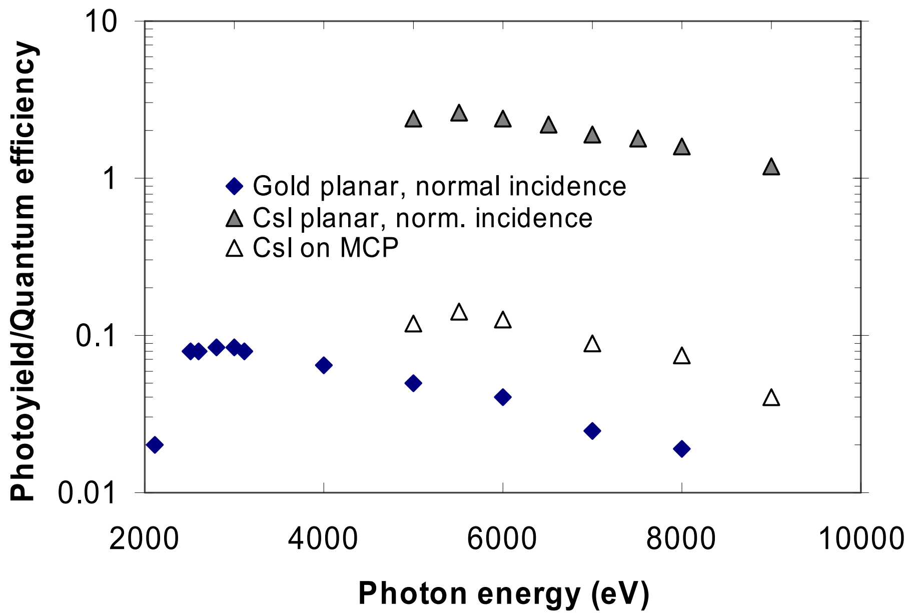

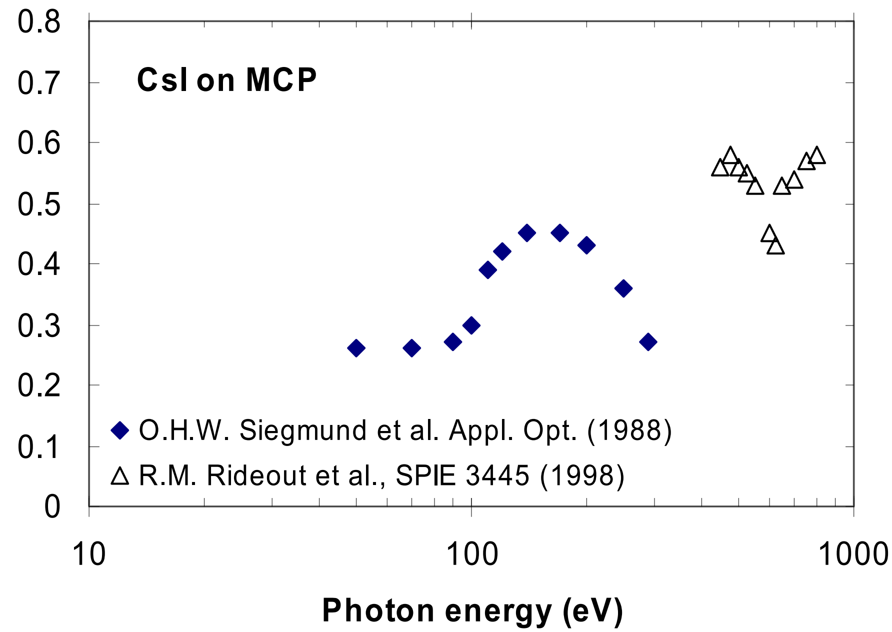

G.W. Fraser et al., NIM A321, A381, SPIE 3445

QE of diamond photocathodes. Reflective mode only

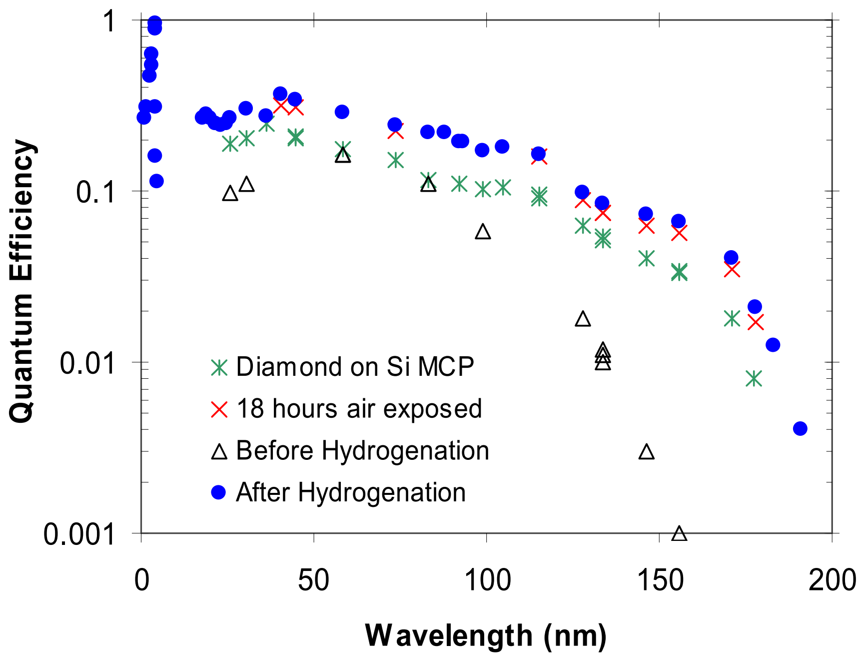

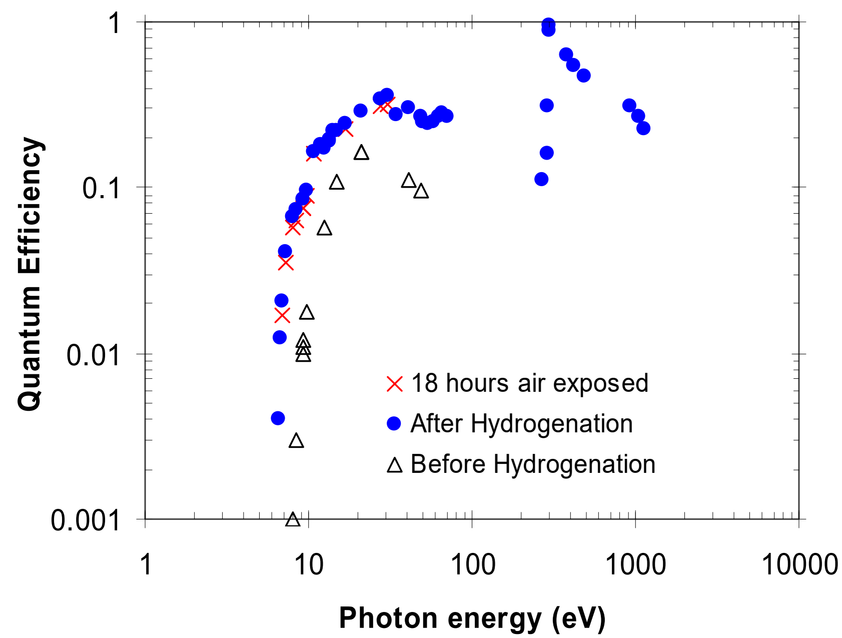

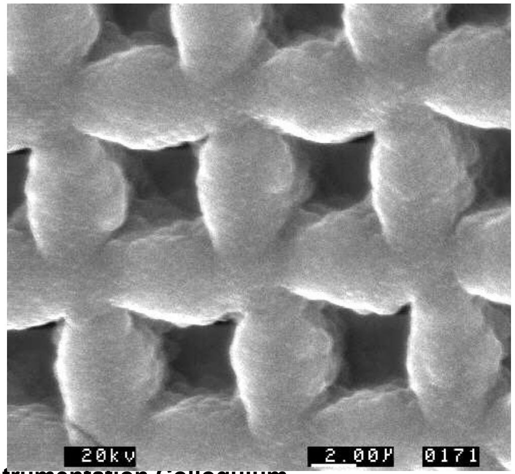

Small grain polycrystalline diamonod photocathode deposited on Si MCP

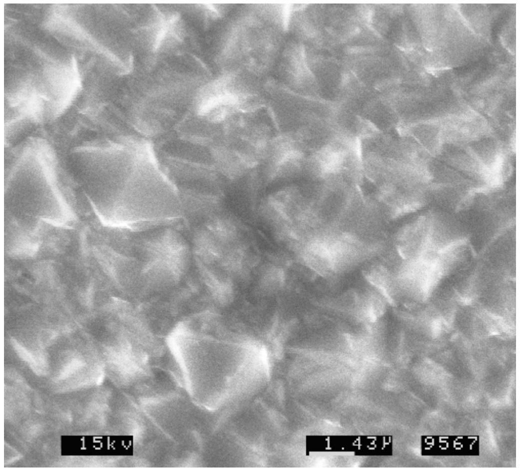

QE of diamond photocathodes

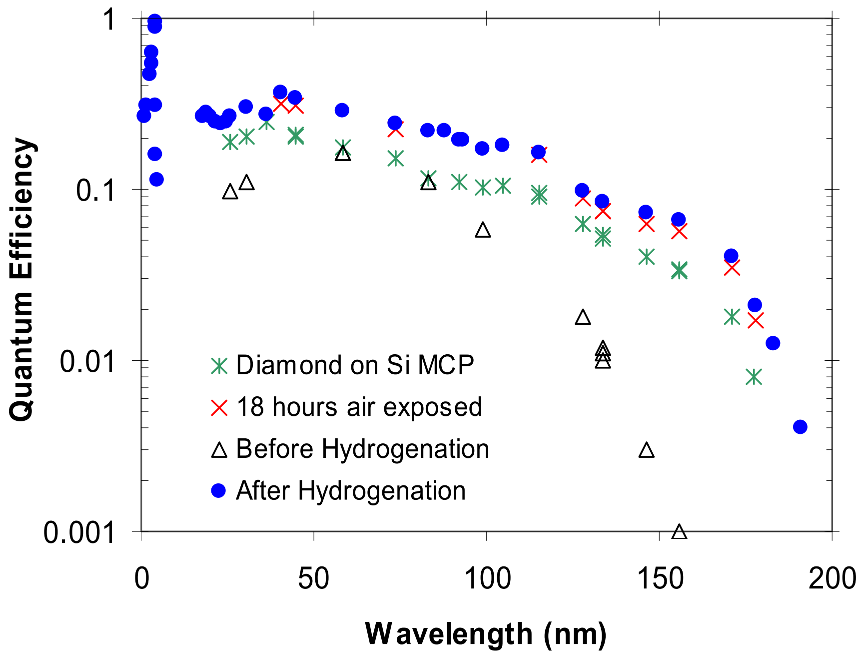

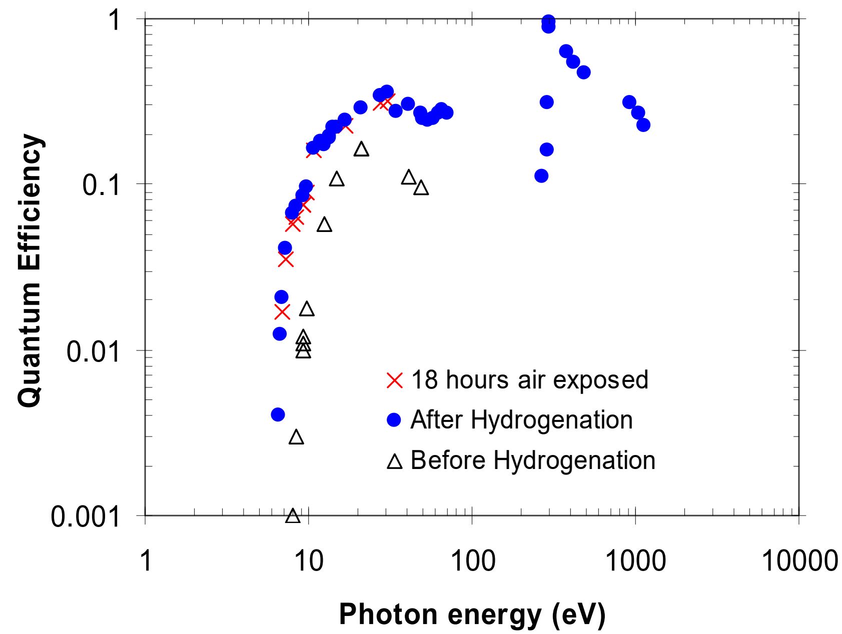

GaN photocathodes

- MBE, MOCVD tried so far, ALD is being tried.
- High quality films require ~800 C deposition temperatures: not compatible with lead glass MCP (can only sustain ~350 C).
- C-plane sapphire crystal matches the GaN lattice. Other substrates tried (MgF, metals) with limited success.
  Recent results from U. Washington on the metals (J.Buckley et al.) are encouraging.
- Naturally grown GaN is n-type. P-type doping is needed.
- Depth-graded doping is required for high QE.

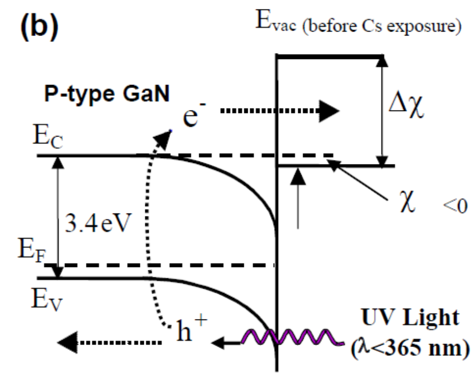

A.M.Dabiran, et al., SPIE 7212-38 (2009)

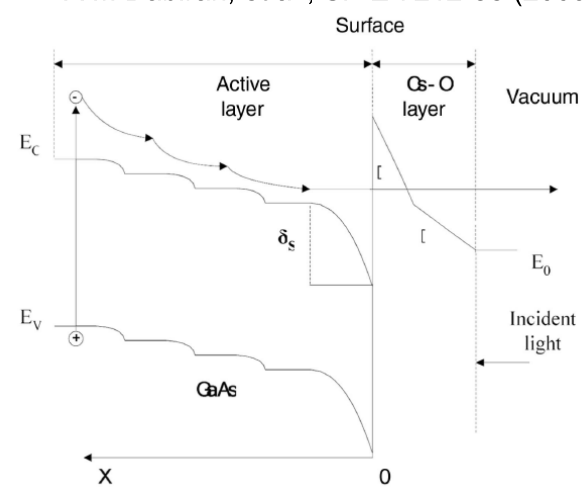

Zhi Yang, et al., Applied Optics 46 (2007) 7035

Activation of GaN films

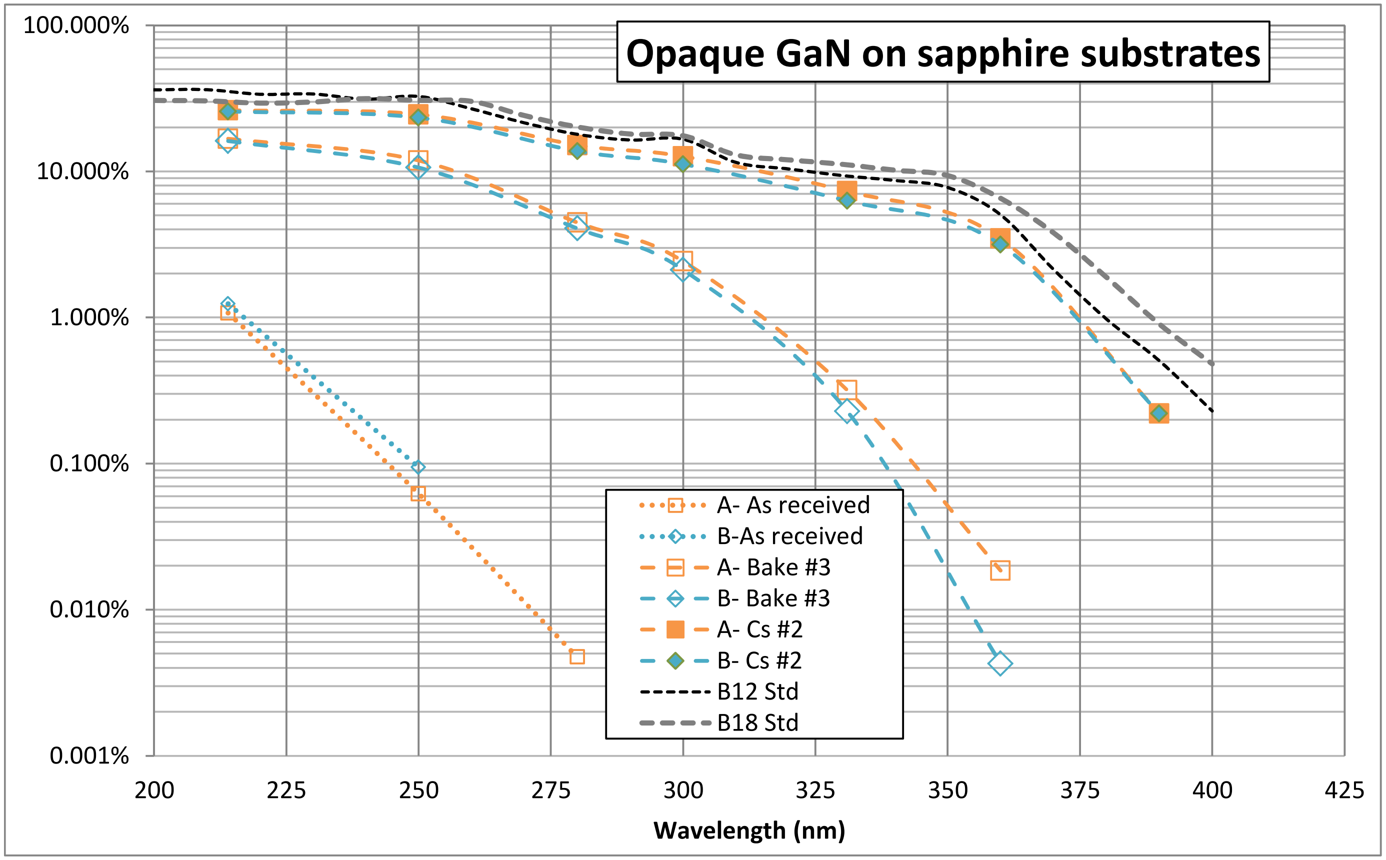

Opaque samples could be reactivated to high QE even after oxygen leak during 350 C baking.

Proc. SPIE Vol 7732, 77324T (2010)
Proc. of SPIE Vol. 8859, 88590X (2013)

GaN Photocathode developments

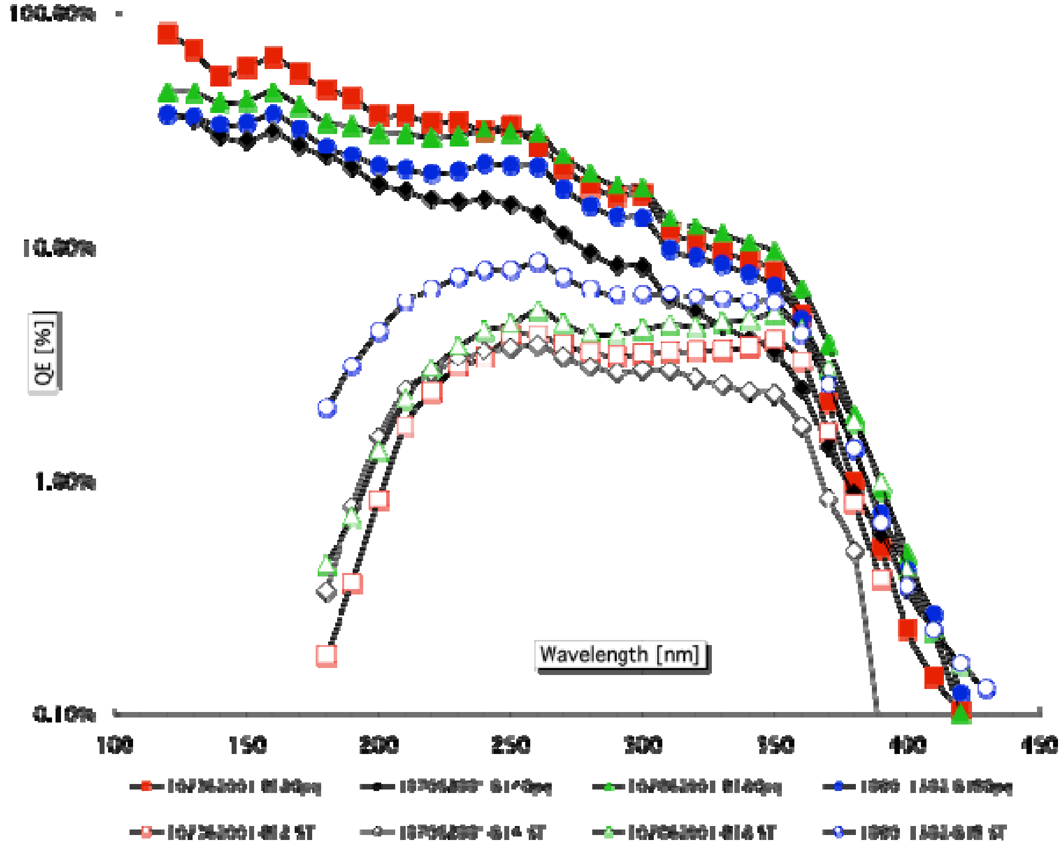

GaN semitransparent and opaque photocathode quantum efficiencies for sample 07062001. GaN is 150nm thick with depth graded Mg concentration. Curves represent different processing conditions. (cleaning methods, heat treatment, and Cesiation processes).

Novel MCPs manufacturing technology enabling novel applications

Nano-engineered MCPs: borosilicate glass and plastic

Micro-capillary arrays (Incom) made with borosilicate glass.
L/D typically 60:1 but can be much larger.
Open area ratios from 60% to 83%.
No etching is needed.
Resistive and secondary emissive layers are applied (Arradiance, Argonne Lab) to allow these to function as MCP electron multipliers.

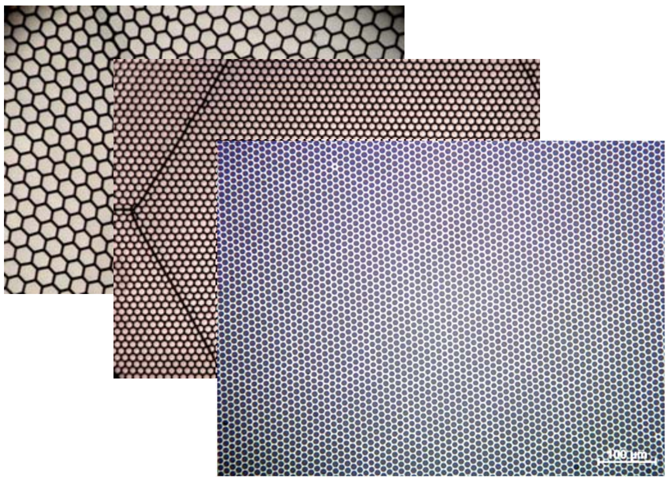

40μm pore borosilicate micro-capillary MCP with 83% open area.

O.H.W. Siegmund, et al.,
Proc. of SPIE Vol. 8859, 88590Y (2013);

Many publications at LAPPD collaboration reference list

Plastic MCPs (Arradiance) made from PMMA.
L/D typically 100:1, 50 μm pores.
Resistive and secondary emissive layers are applied by Atomic Layer Deposition (Arradiance)

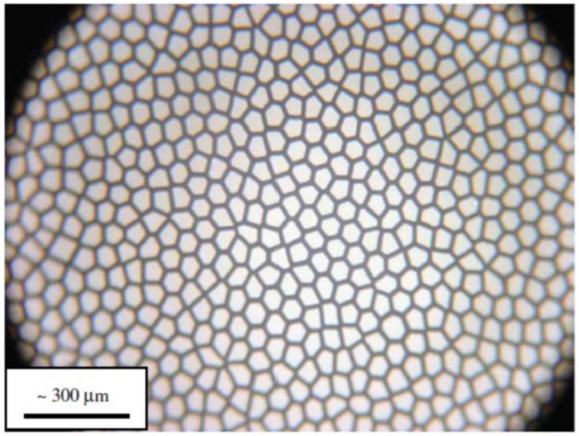

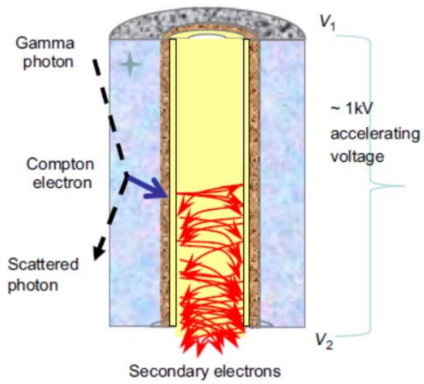

D.R. Beaulieu et al., Nucl. Instr. Meth. Phys. Res. A 659 (2011) 394–398

ALD / Borosilicate Glass MCPs

Fabricated using hollow tube draw and stack technique

Glass is inexpensive, low Z (no lead), higher softening temperature (>700° C)

- *Lower gamma background, low high energy particle cross section*
- *Deposition of high Temp opaque photocathodes like GaN*
- *Very large formats (>20cm) are possible*

Functionalized using Atomic Layer Deposition (ALD)

- *Semiconductor Resistive layer, tunable over wide range*
- *Amplifying layer (e.g. Al_2O_3 or MgO) with high secondary electron coeff.*
- *Better lattice match to GaN, also good for conventional cathodes*
- *Can be used on conventional MCPs and MCP substrates*

Separates MCP functional properties from substrate optimization!

O.H.W. Siegmund, et al., Proc. of SPIE Vol. 8859, 88590Y (2013)

Imaging 20cm, 20μm pore ALD-MCP Pairs

A number of 20cm MCP substrates have been functionalized by ALD at ANL, and put through detailed tests at UCB-SSL .

Expanded area view showing the mutifiber edge effects.

Pulse height distributions for UV and background.

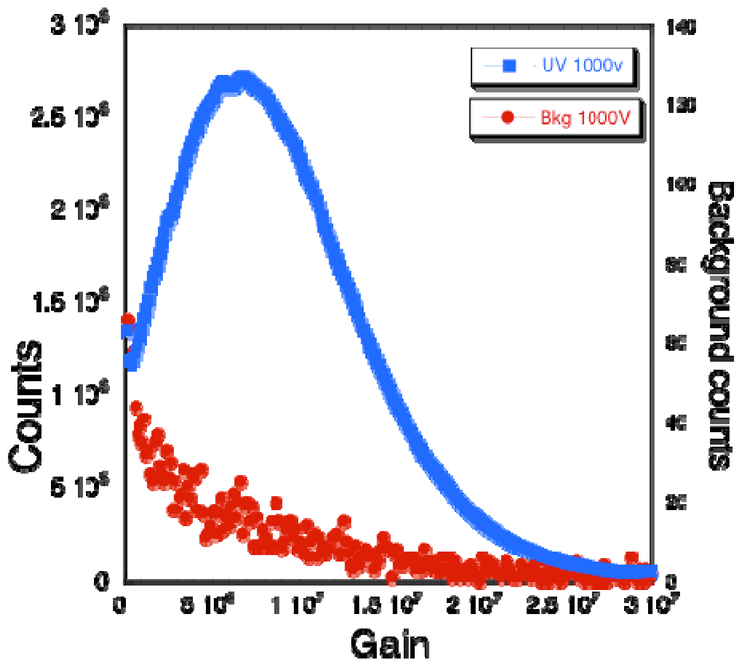

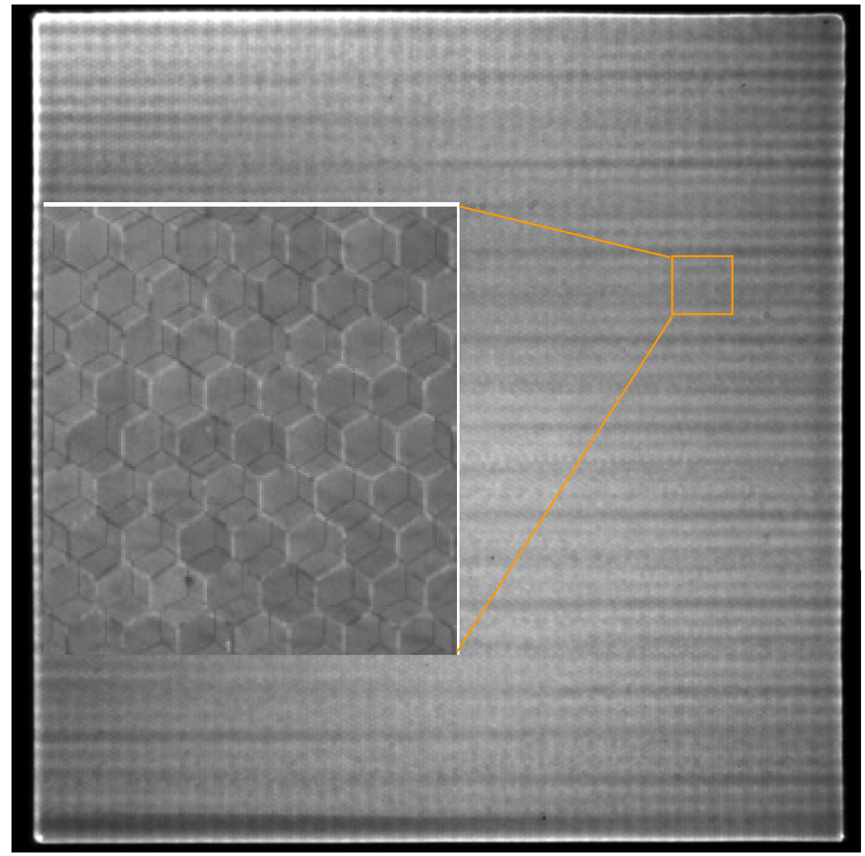

Image striping is due to the anode period modulation as the charge cloud sizes are too small for the anode. 20cm, 20μm pore, Al_2O_3 SEY, MCP pair image with 185nm non uniform UV illumination.

Stability of MCP: new technology of MCP manufacturing

- MCP scrubbing/preconditioning is a well known problem with photon detectors, used in very high count rate applications.
- Novel technology of MCP manufacturing has solution for it (not done for neutron-sensitive MCPs yet).
- **Improved lifetime of microchannel-plates**

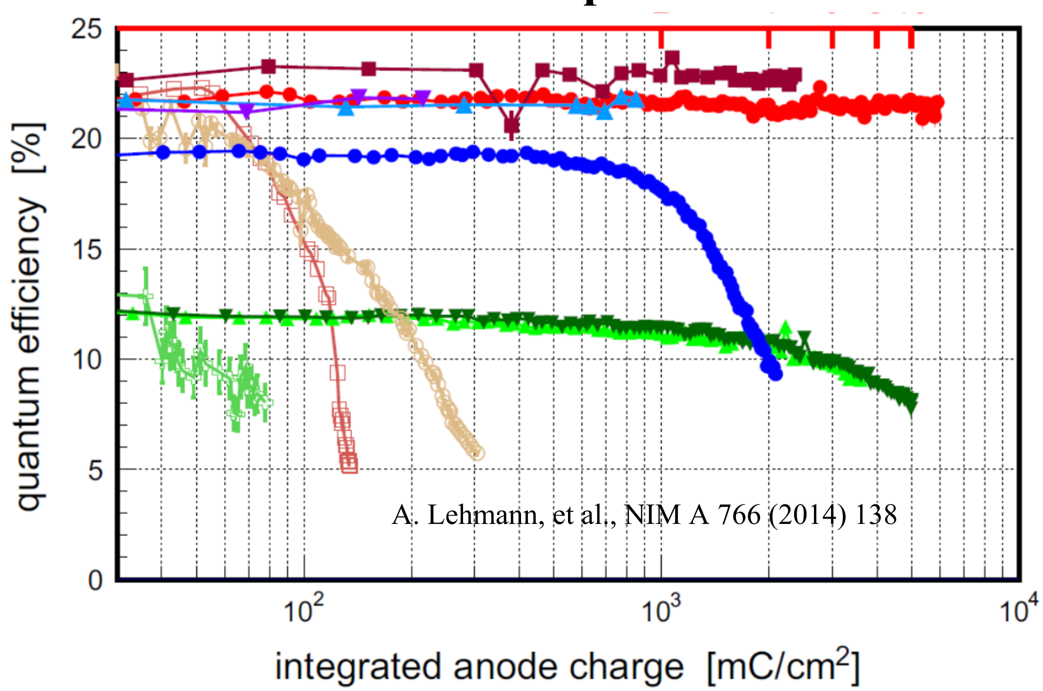

D.R. Beaulieu et al., NIM A 607(2009) 81
O.H.W. Siegmund, et al, NIM A 787 (2015) 110

Neutron sensitive MCPs: ^{10}B doped glass

Nova Scientific, Inc, MA, USA produces $^{10-}$B doped glass MCPs
Novel non-destructive testing applications become possible

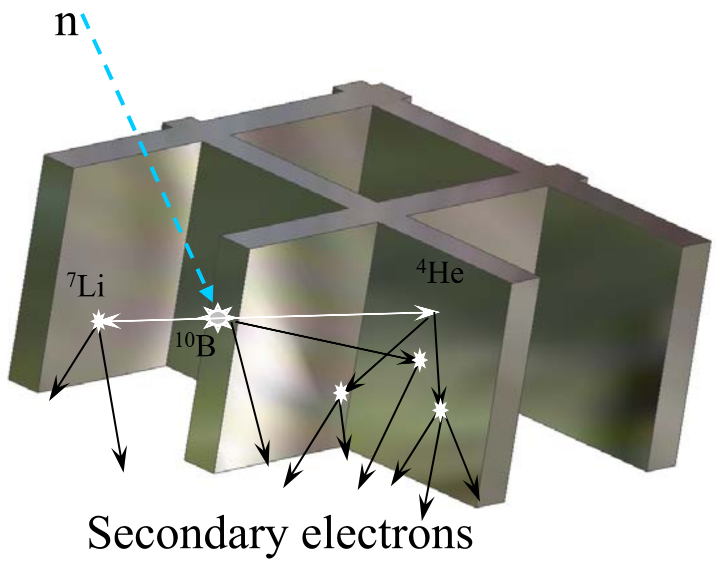

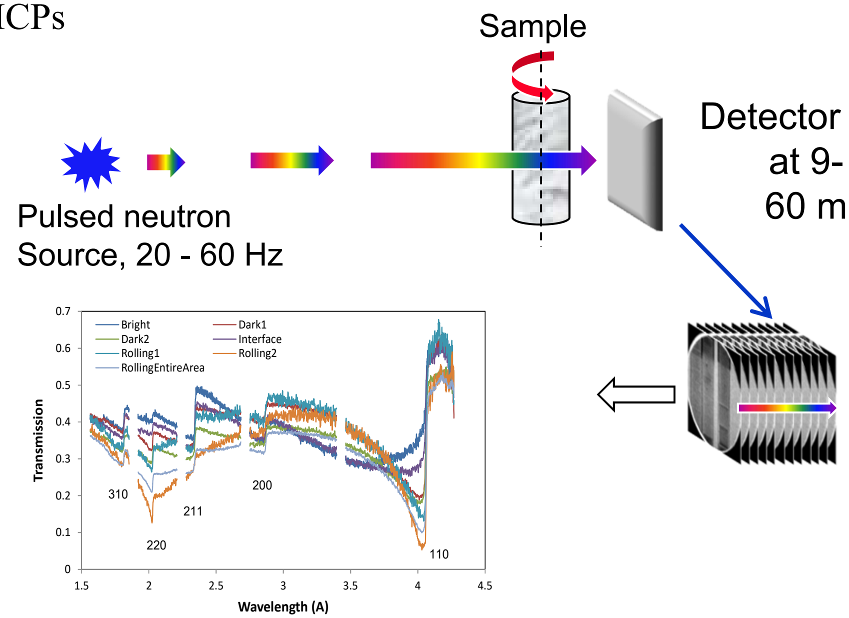

TOF = neutron energy
>250000 spectra measured at the same time

~8 µm pores on 11 µm centers, L/D ~100:1
Detection efficiency > 50 % for thermal neutrons

A.S. Tremsin et al., Nucl. Instr. Meth. Phys. Res. A 539 (2005) 278-311

Neutron attenuation coefficient

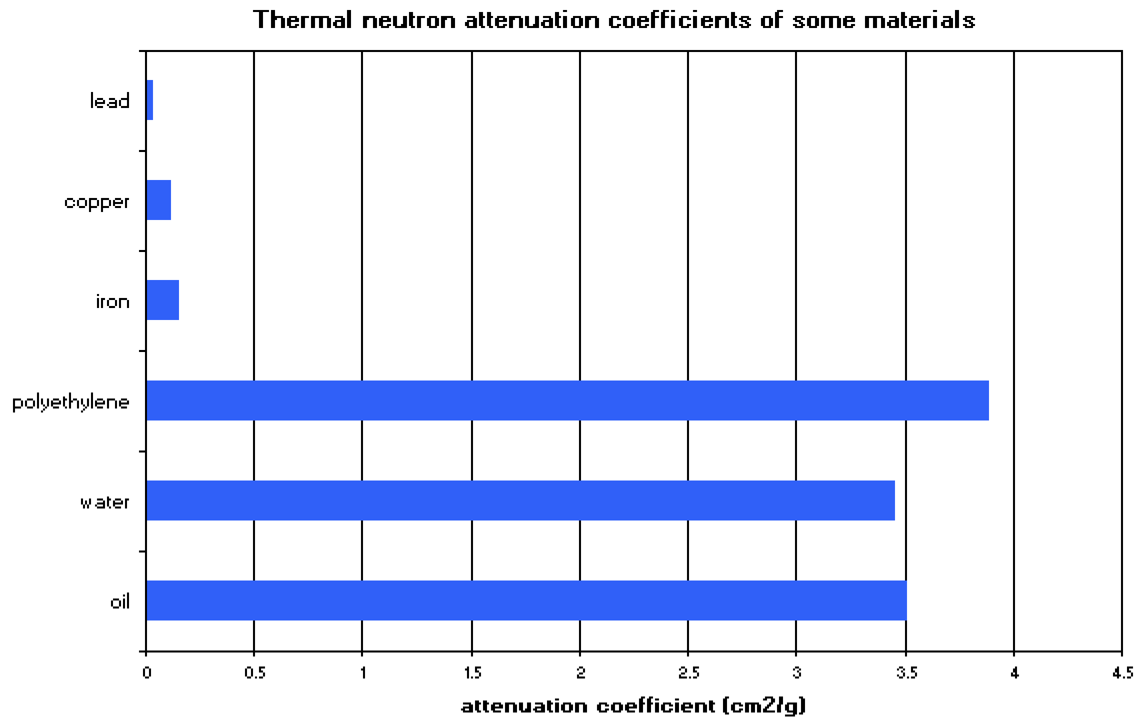

Source: Paul Scherrer Institute website

500 years old buddha: X-rays versus neutrons

Photo of the buddha
height about 20 cm

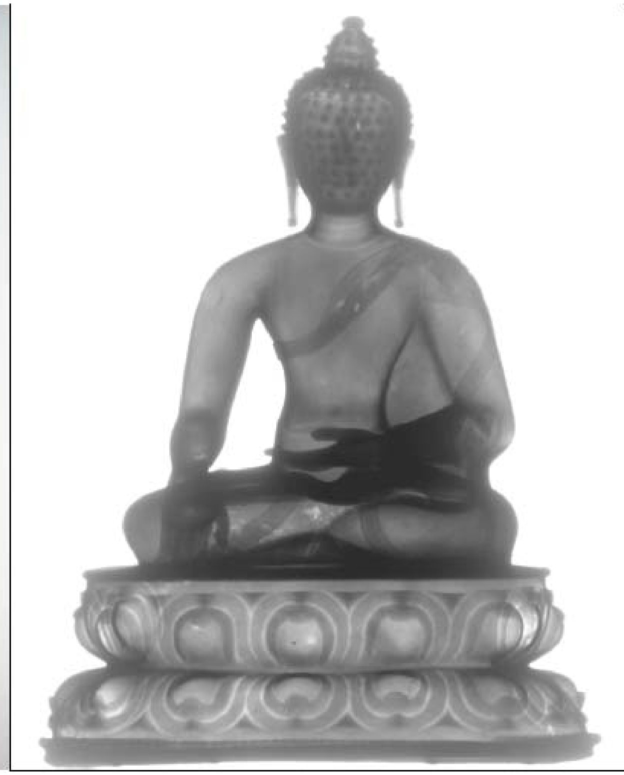

150 kV X-ray

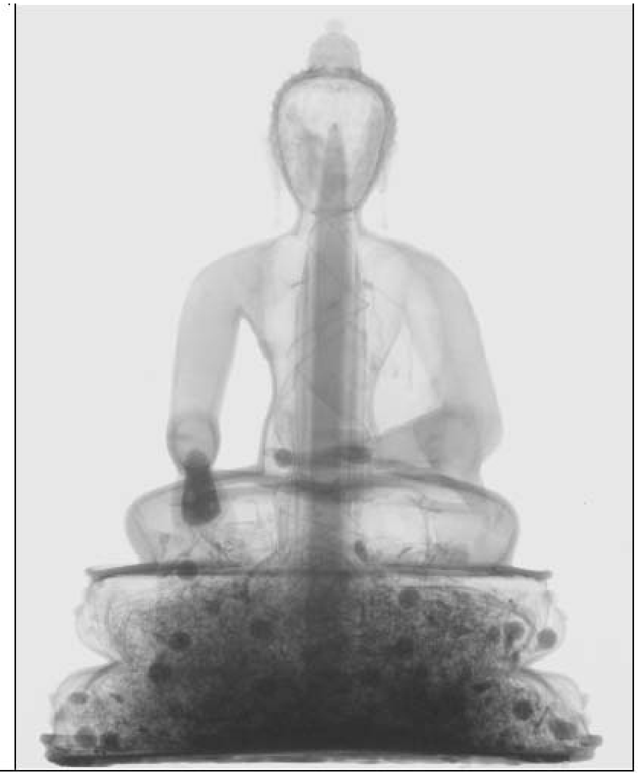

Thermal neutrons

The organic material content (wood, dry flowers, paper, cord) are only accessible in a non-invasive way using the neutron imaging option.

E. H. Lehmann, et al., Journal of Instrumentation, JINST 6 C01050 (2011)

Conventional neutron radiography

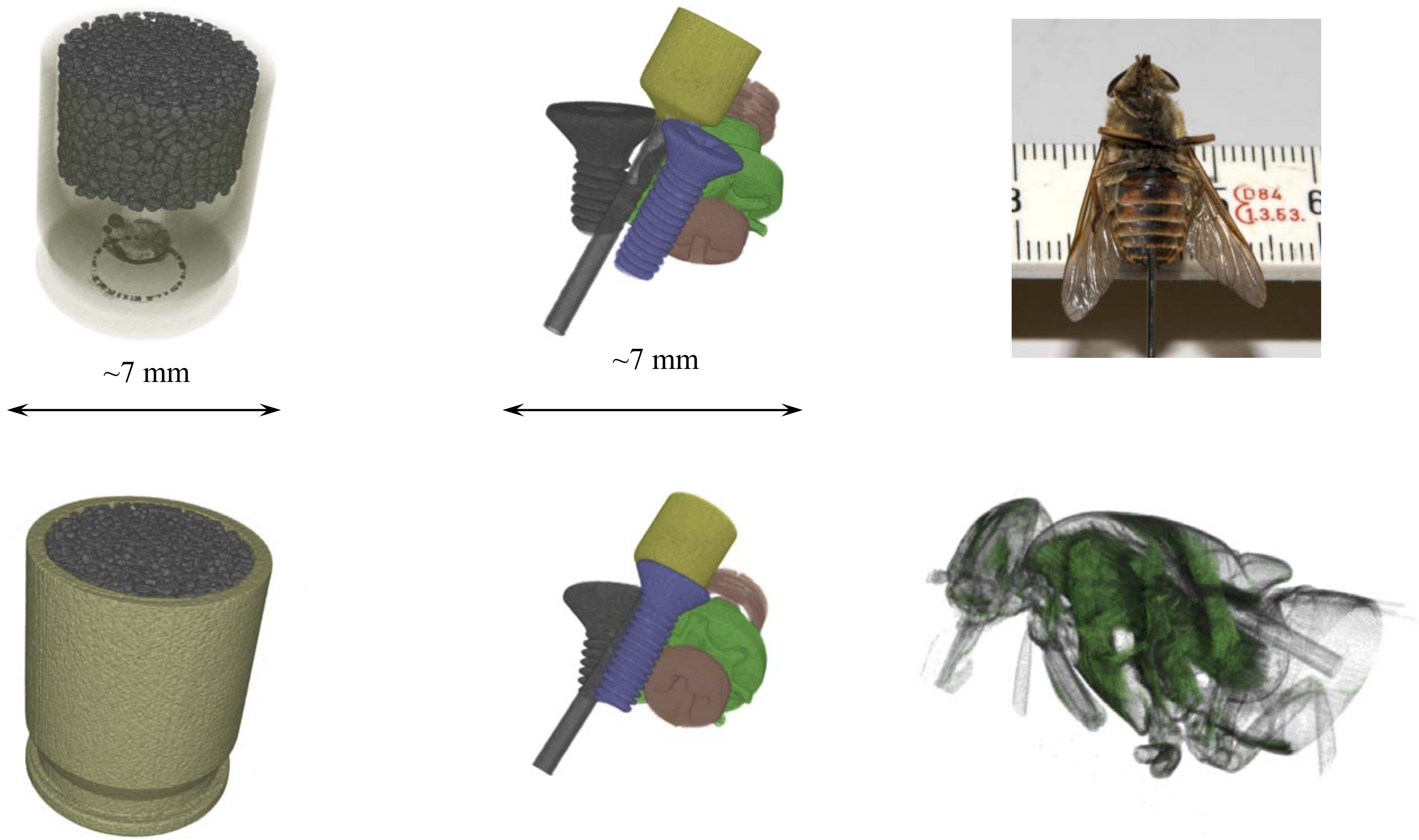

Nucl. Instr. and Meth. A 652, pp.400-403 (2011).

Measurement of strain

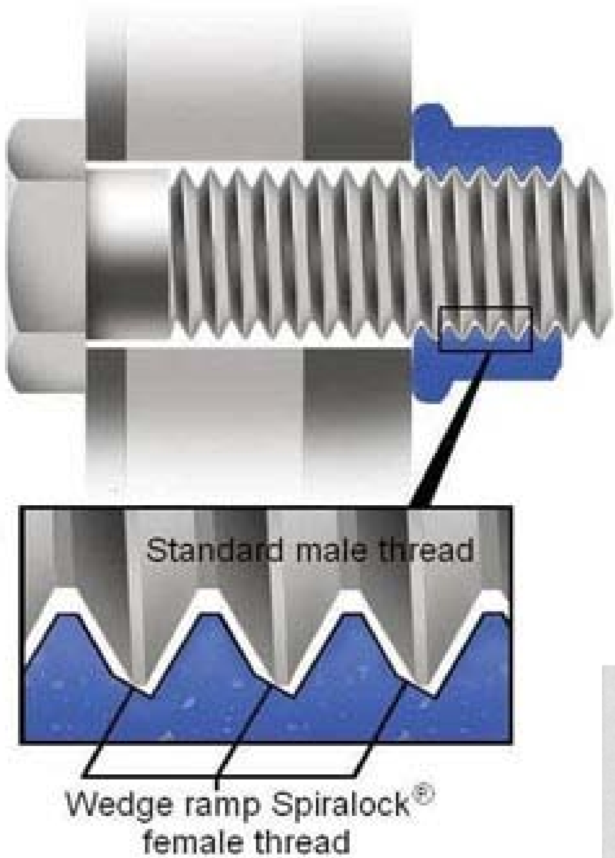

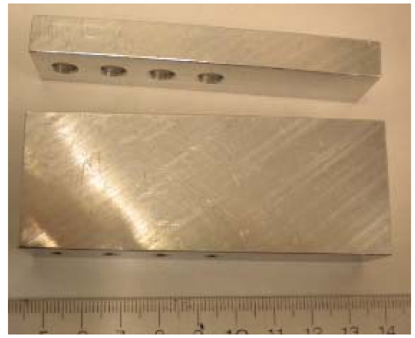

Steel screws in Al base

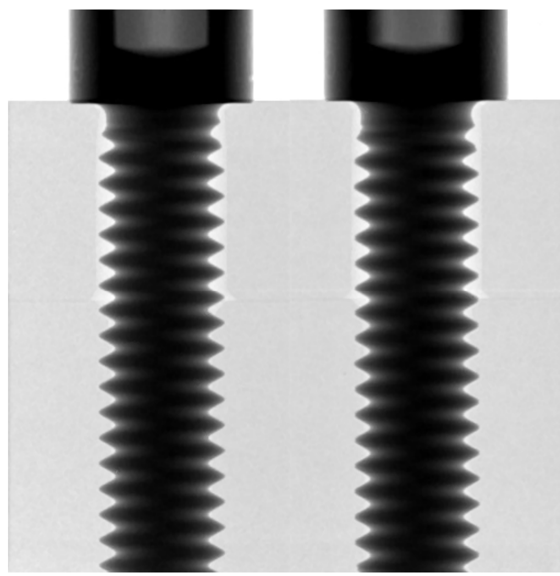

Steel screws in stainless steel

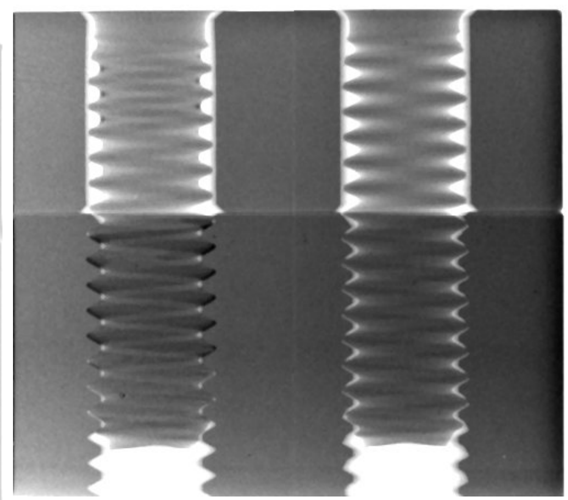

Load in Spiralock threads

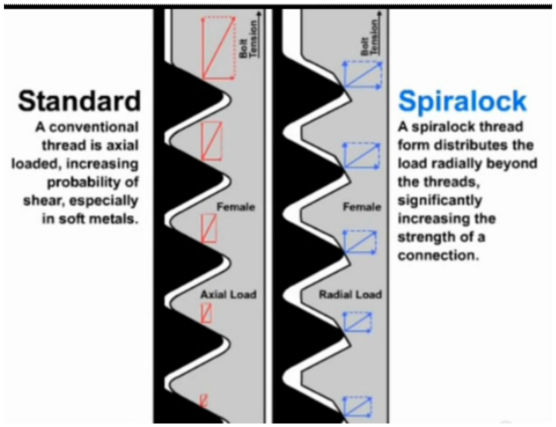

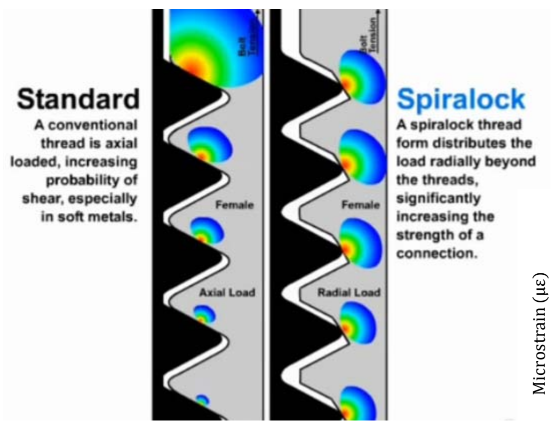

Torqued to 185 lb-in

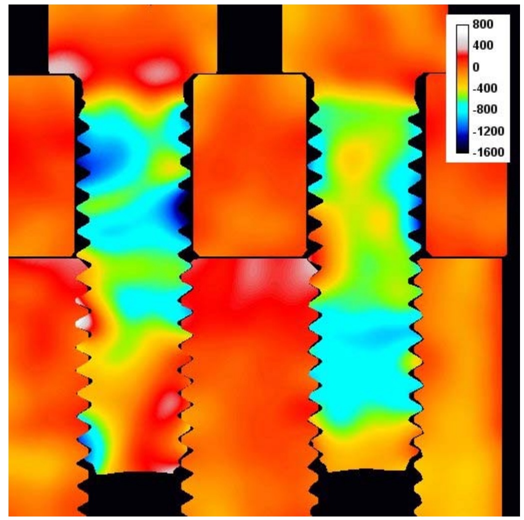

Not torqued

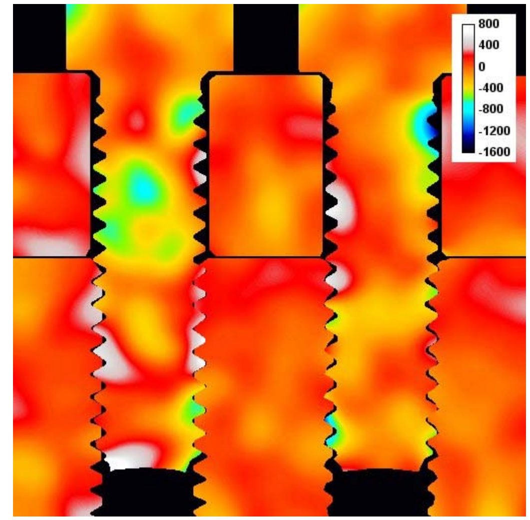

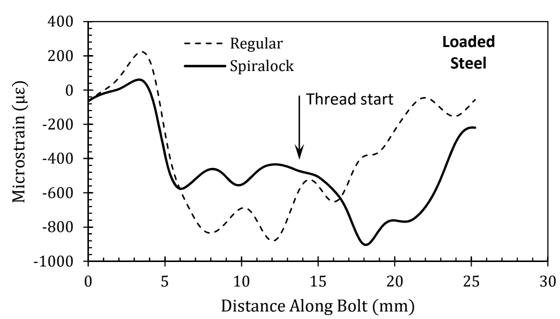

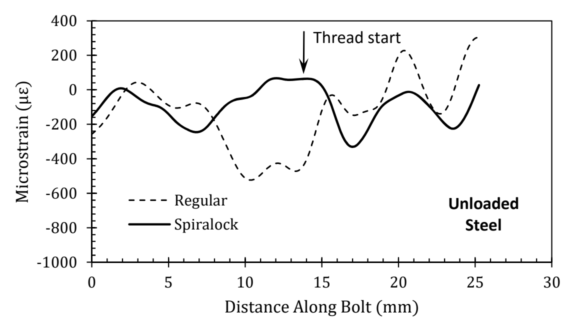

A.S. Tremsin et al., *Non-destructive examination of loads in regular and self-locking Spiralock® threads through energy-resolved neutron imaging,* In print Strain, July 2016

In situ imaging of crystal growth

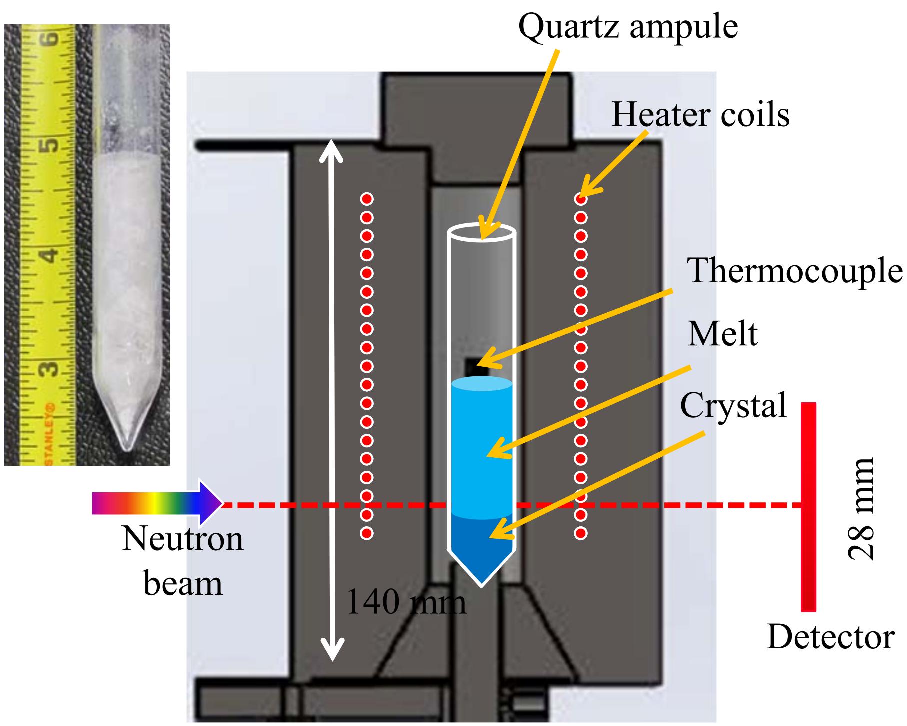

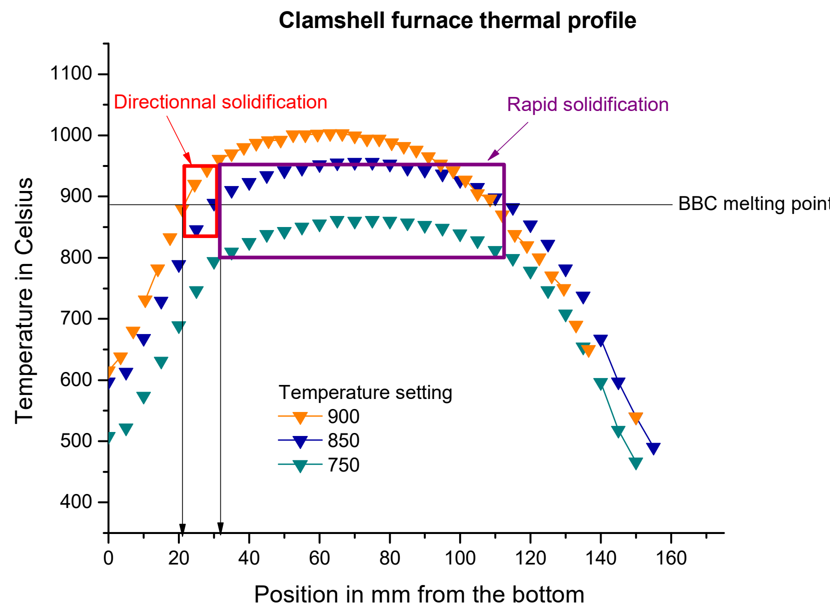

Lawrence Berkeley National Laboratory: E. D. Bourret-Courchesne, G. A. Bizarri, D. Perrodin, I. Khodyuk, T. Shalapska

supported by the U.S. Department of Energy/NNSA/DNN R&D and carried out under Contract NO. AC02-05CH11231a

Experimental setup pulsed beam; energy resoled imaging

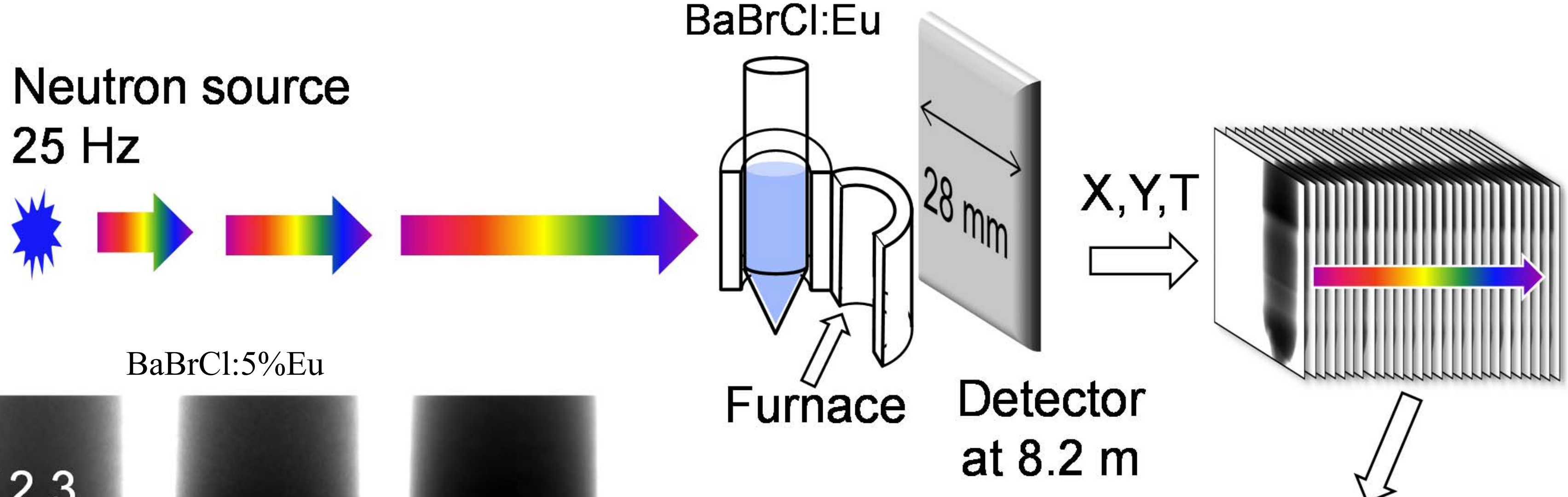

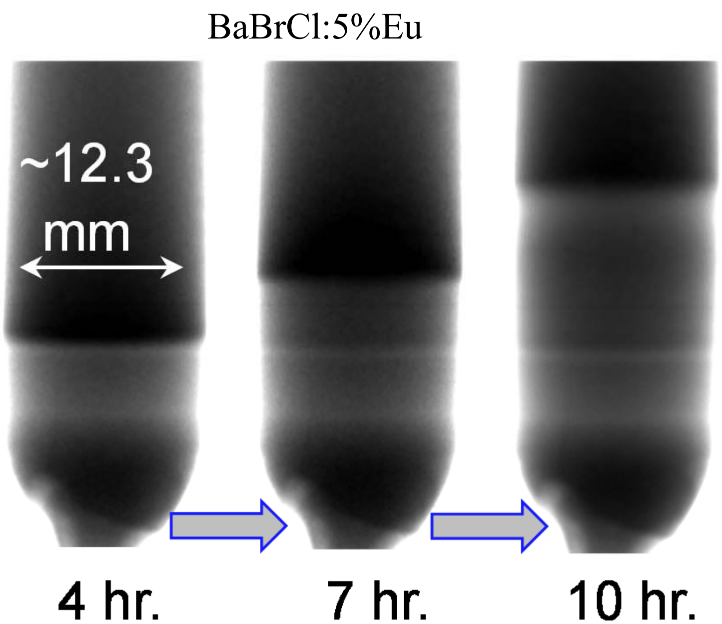

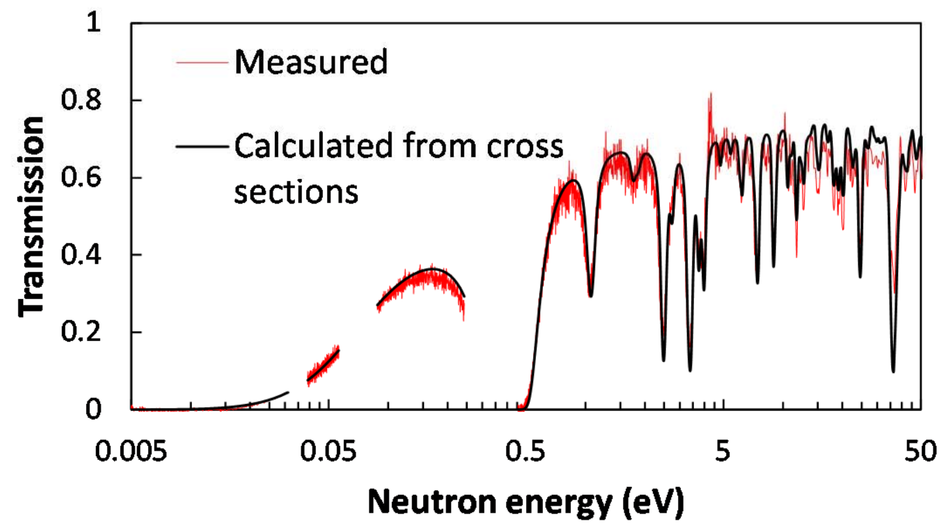

Lawrence Berkeley National Laboratory: E. D. Bourret-Courchesne, G. A. Bizarri, D. Perrodin, I. Khodyuk, T. Shalapska supported by the U.S. Department of Energy/NNSA/DNN R&D and carried out under Contract NO. AC02-05CH11231a

Eu distribution quantification

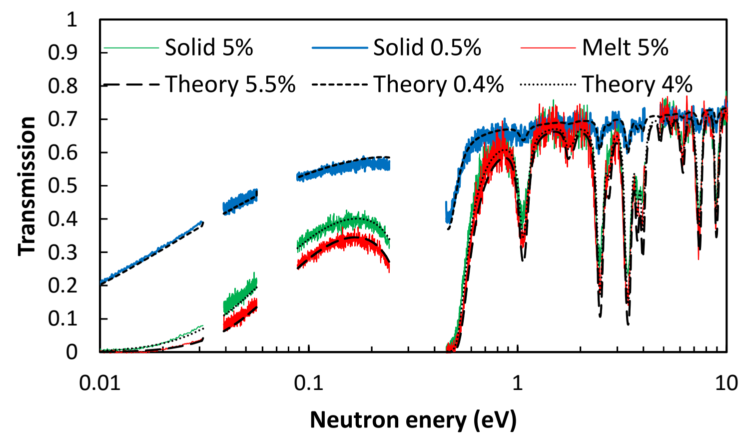

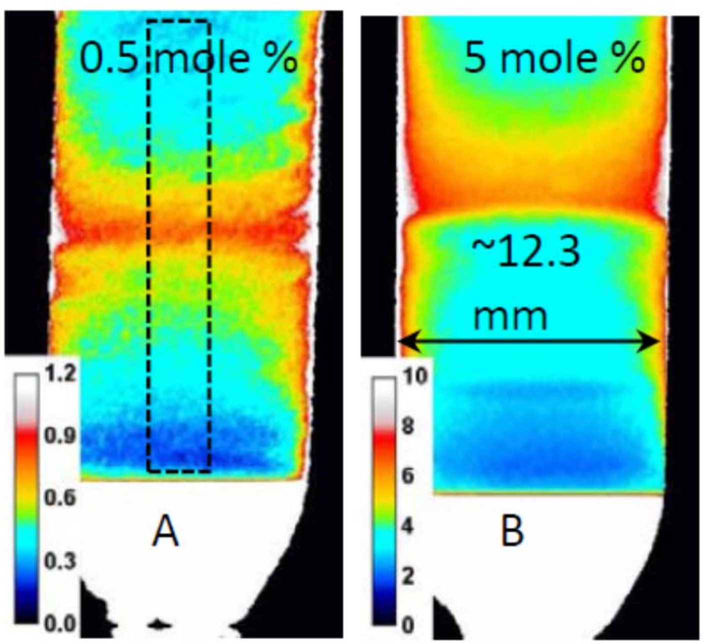

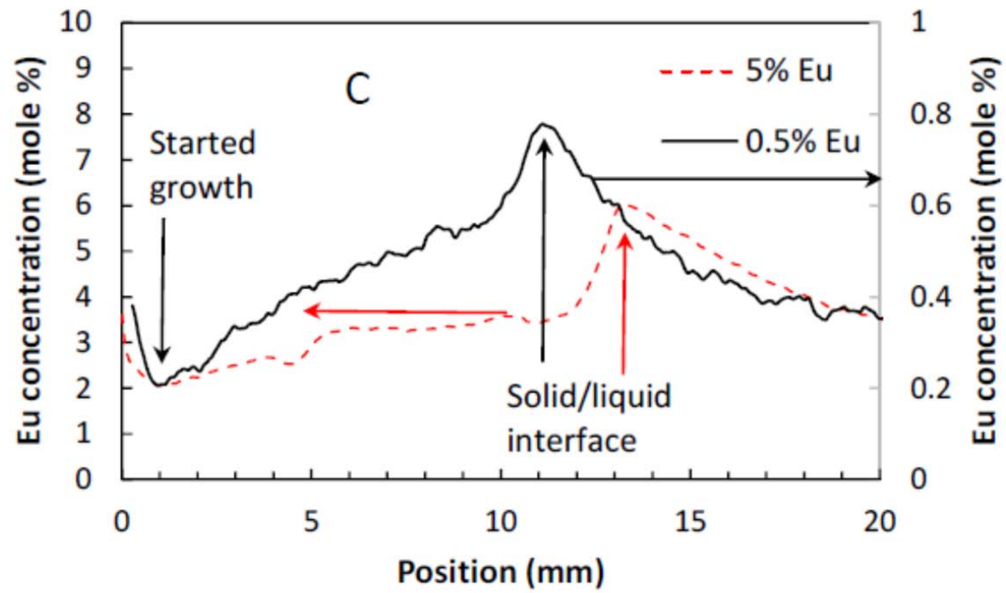

Non destructive examination of Nuclear Fuel Pellets

Changes in nuclear fuels introduced by irradiation

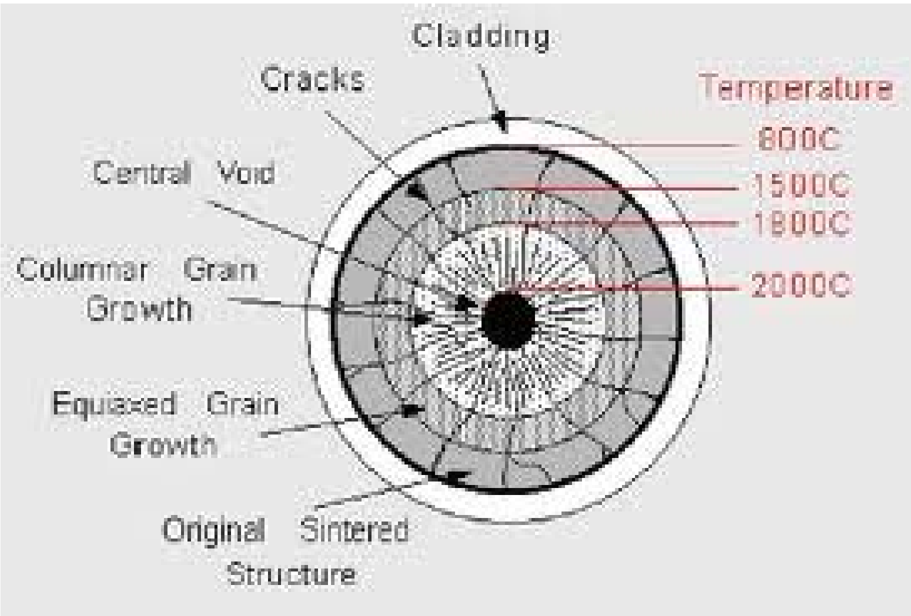

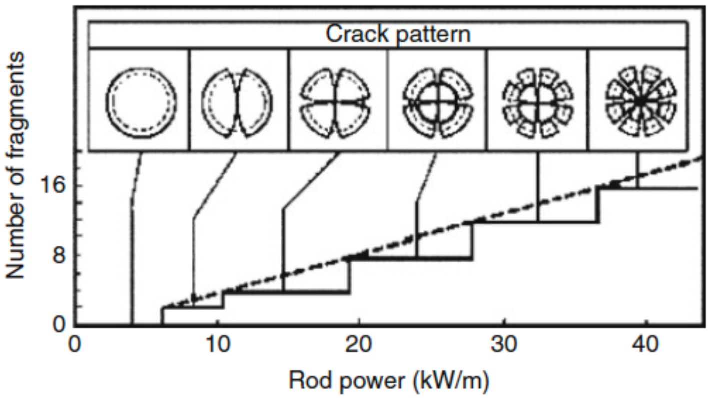

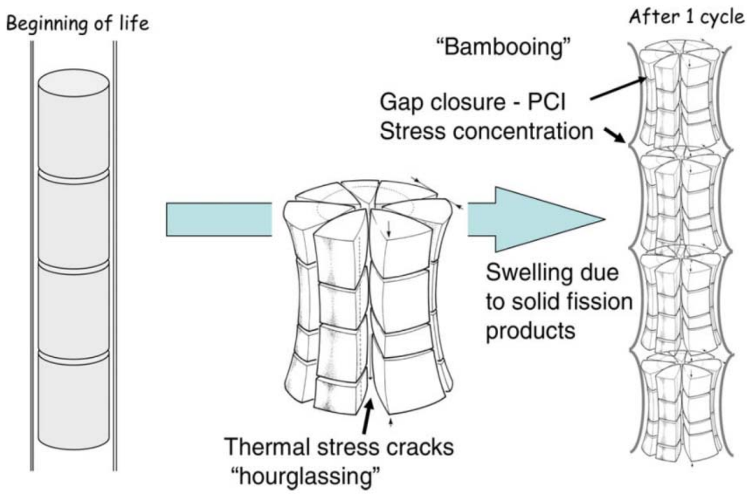

M. Oguma, Nucl. Eng. & Design **76** (1983) 35-45.
D. Olander, J. Nucl. Mat. **389** (2009) 1-22.

Non destructive Examination of Nuclear Fuel Pellets

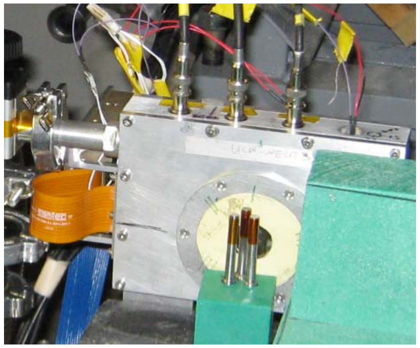

U-238 only
resonance imaging

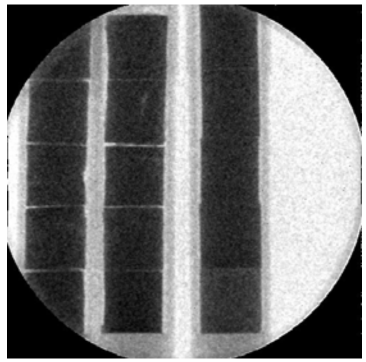

W only resonance
imaging

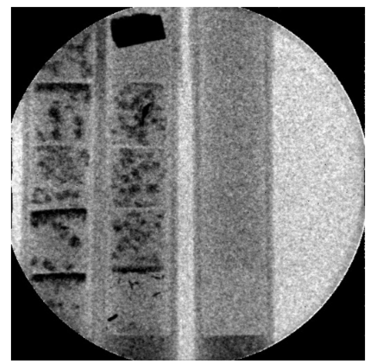

Cracks and voids are
seen through steel
cladding

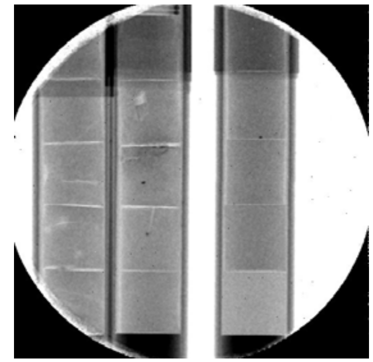

All 3 images obtained simultaneously in one measurement

Los Alamos National Laboratory: S. Vogel, A. Losko, M. Mocko, M.A.M. Bourke, K. McClellan, D. Byler

Journal of Nuclear Materials 440, pp. 633–646 (2013)

Dissimilar welds: SS to Titanium; Al to Steel

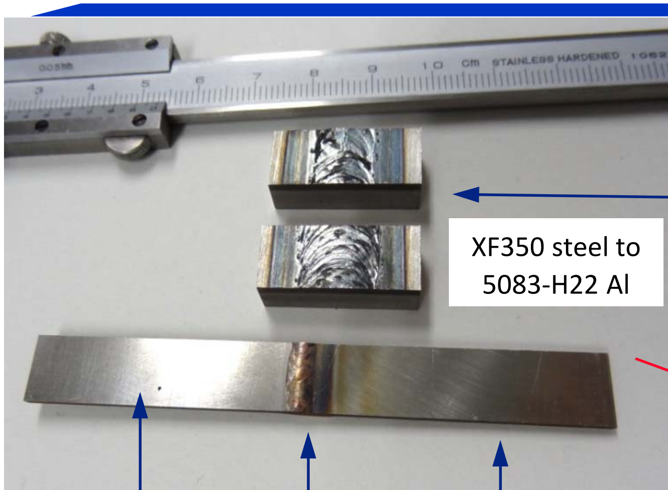

Steel to Al: laser welded

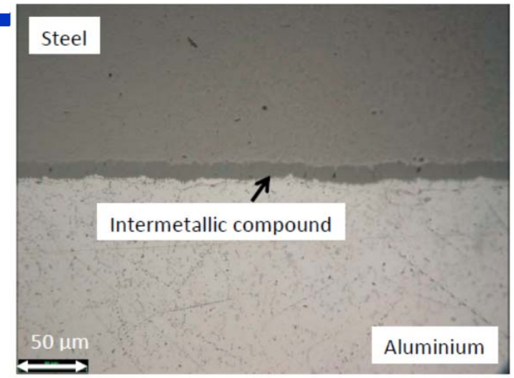

Steel

Copper welding interface

Ti

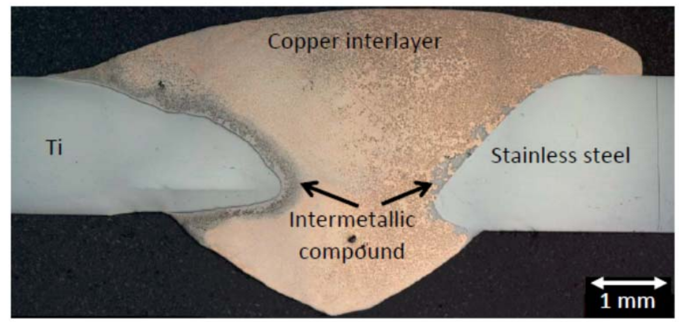

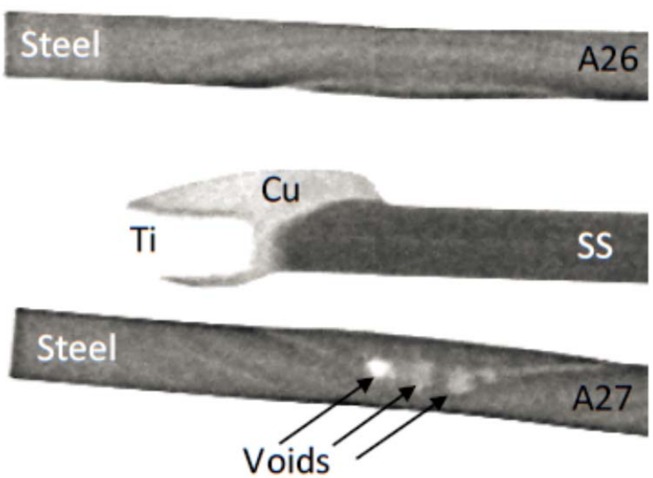

Full spectrum neutron radiography

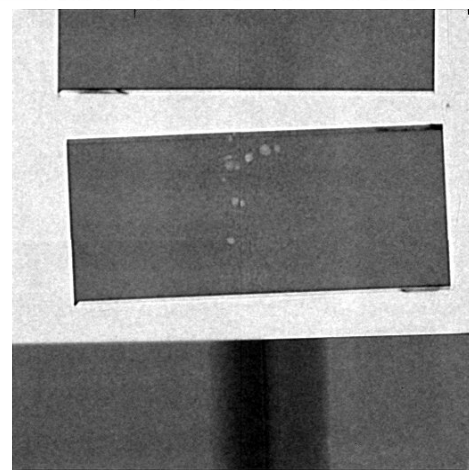

In collaboration with Cranfield Univ.,
J. Appl. Cryst. (2016). 49, 1130-1140; doi:10.1107/S1600576716006725

Dissimilar welds: SS to Titanium; Al to Steel

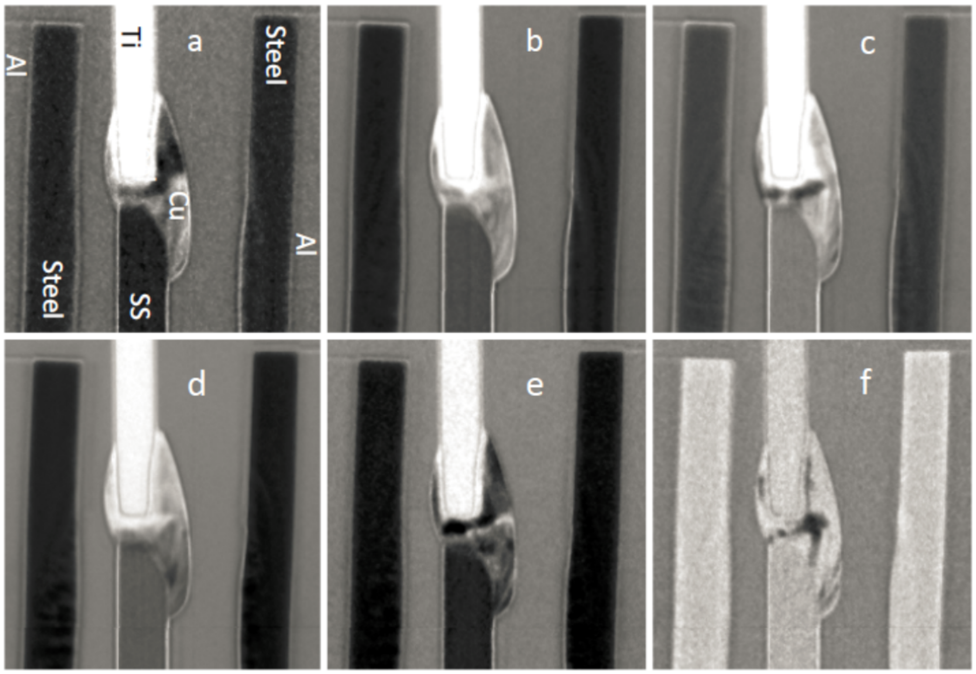

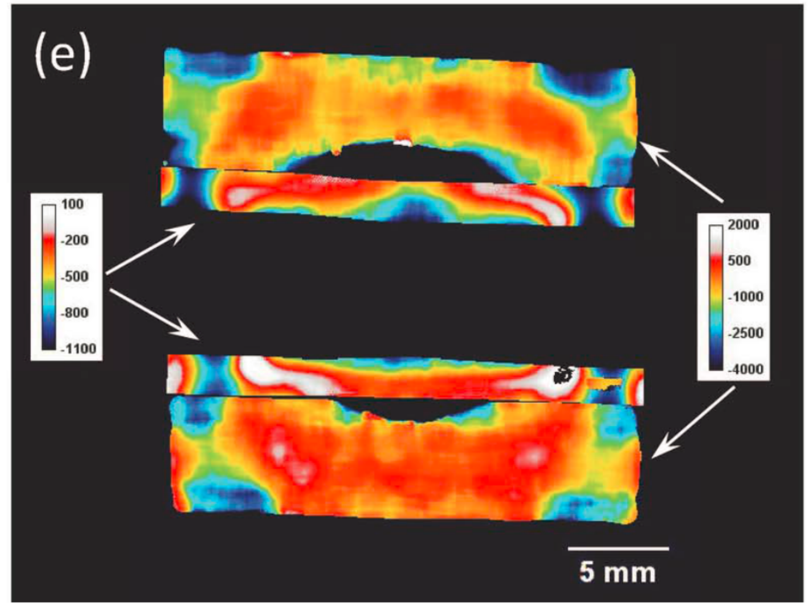

Strain maps and elemental distribution

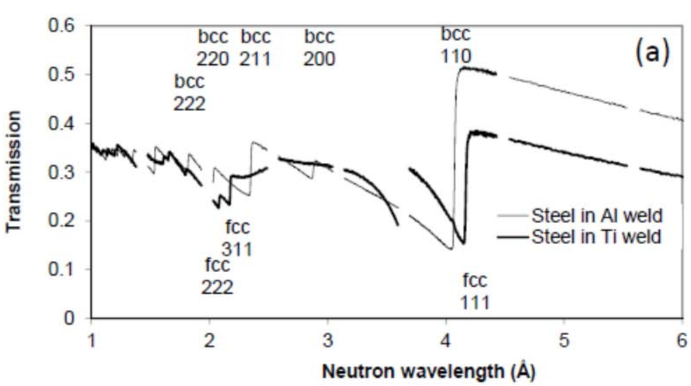

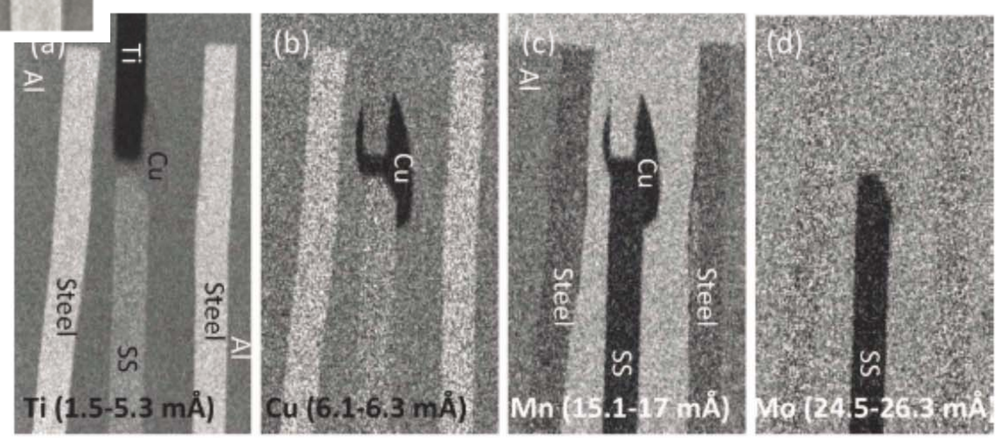

In collaboration with Cranfield Univ.,
J. Appl. Cryst. (2016). 49, 1130-1140; doi:10.1107/S1600576716006725

Water quantification: dynamic studies

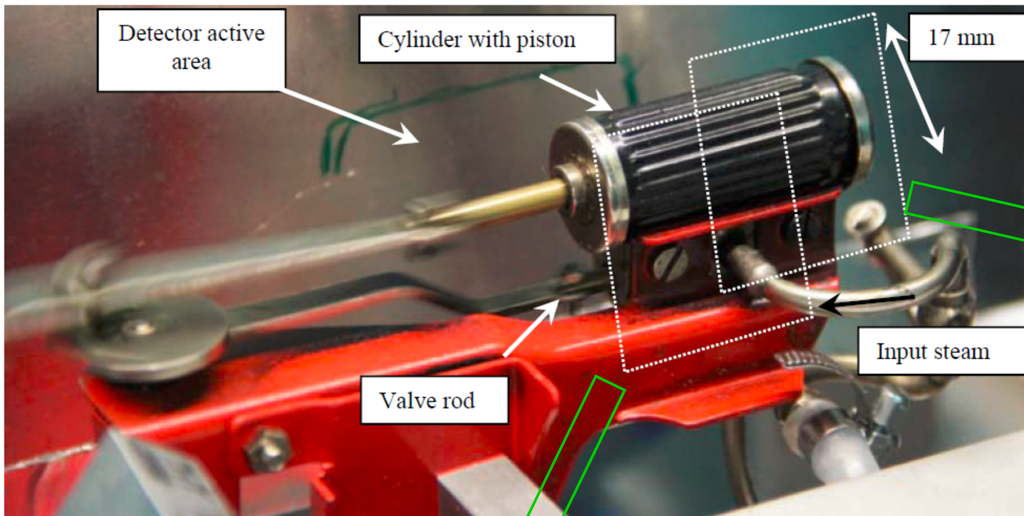

Operation with steam
(1 ms time slice)

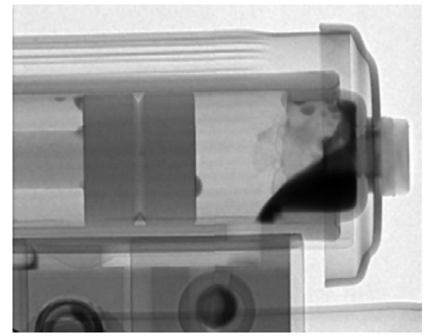

Dry cylinder operation
(1 ms time slice)

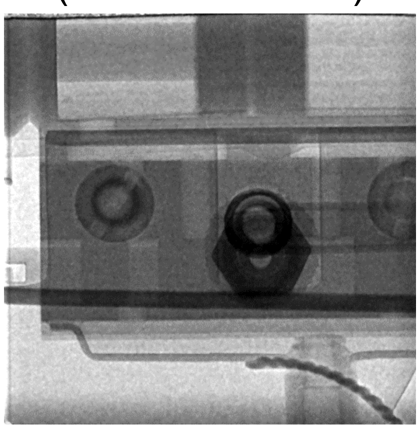

Operation with steam
(1 ms time slice)

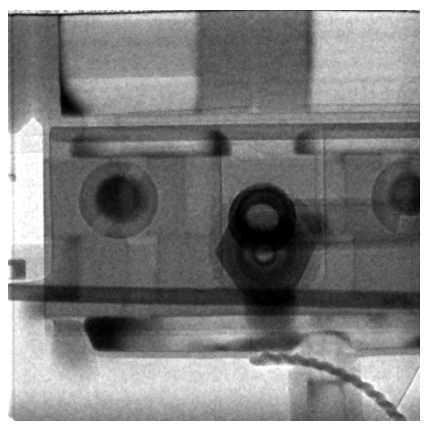

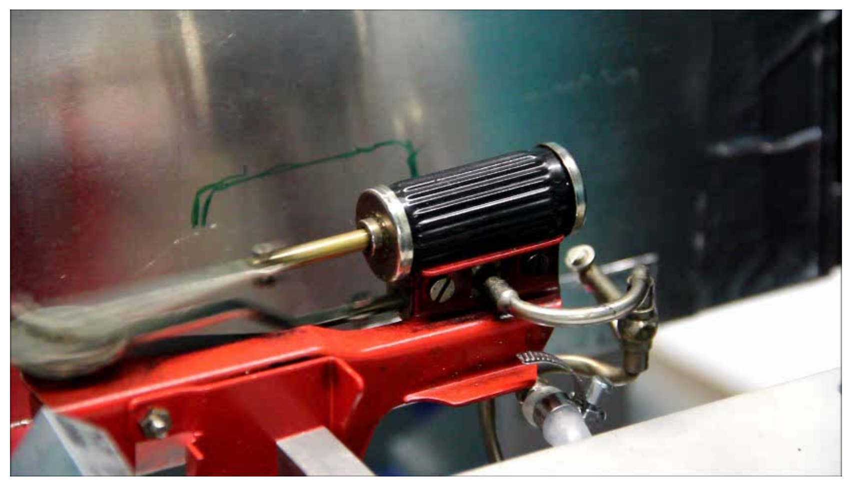

Journal of Instrumentation JINST 10 (2015) P07008

Model seam engine running at 10 Hz

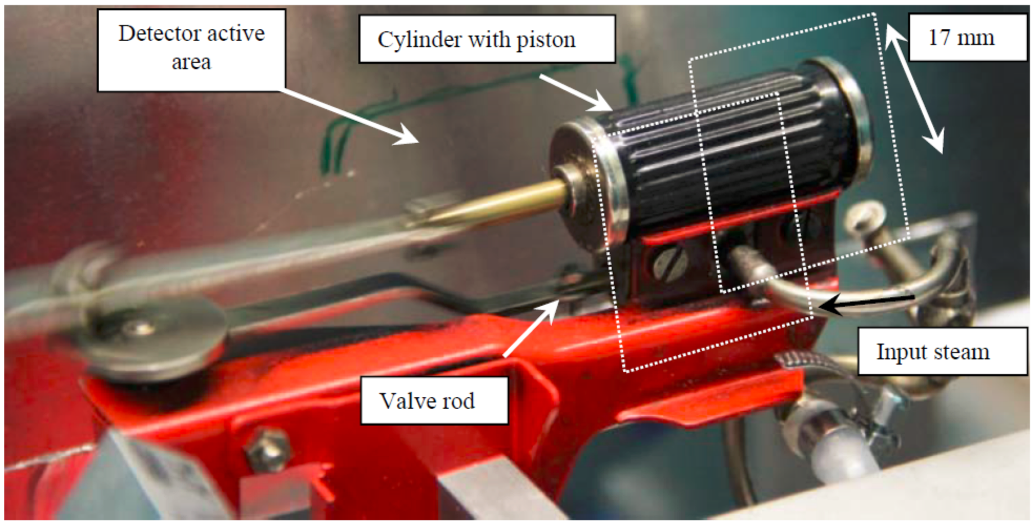

Condensation within the cylinder

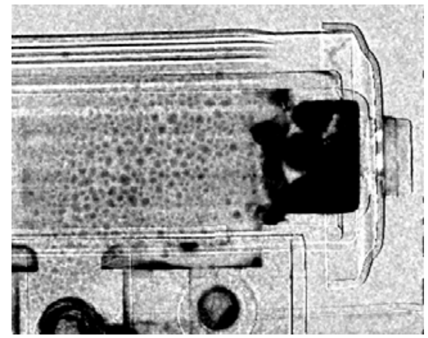

Measured position of the cylinder piston

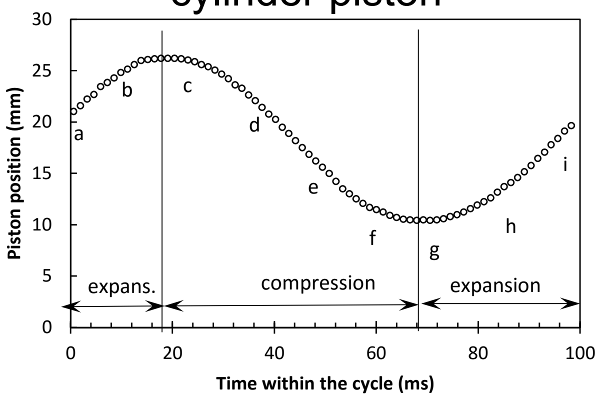

Dry cylinder operation (1 ms time slices)

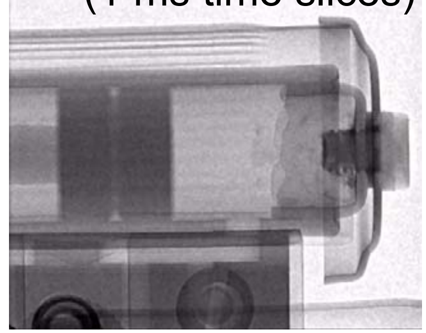

Operation with steam (1 ms time slices)

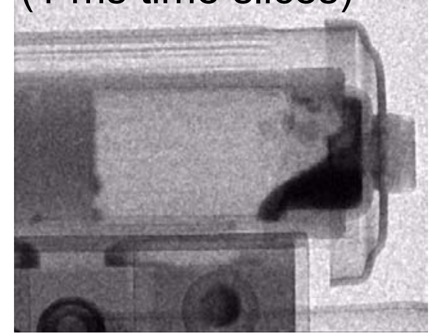

Model seam engine running at 10 Hz

Only water is left in the images

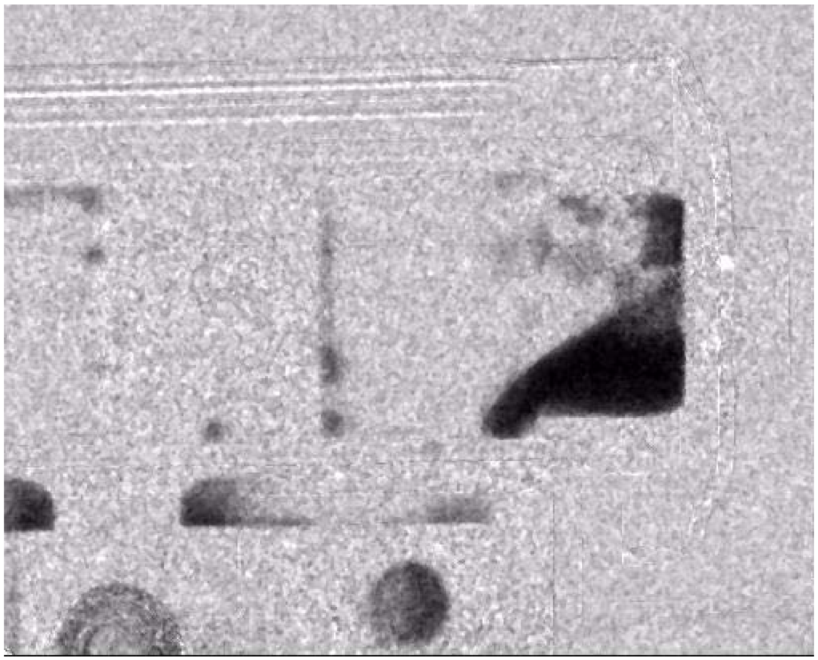

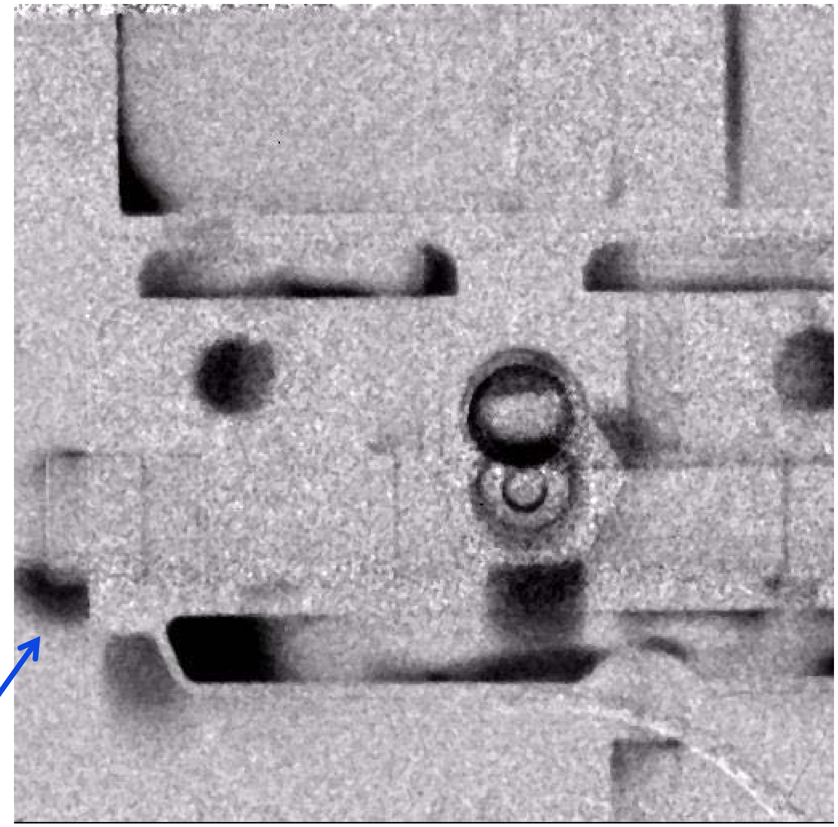

Leaking valve: a droplet
is formed in each cycle

Water quantification as a function of time within the cycle

Water thickness averaged over all phases

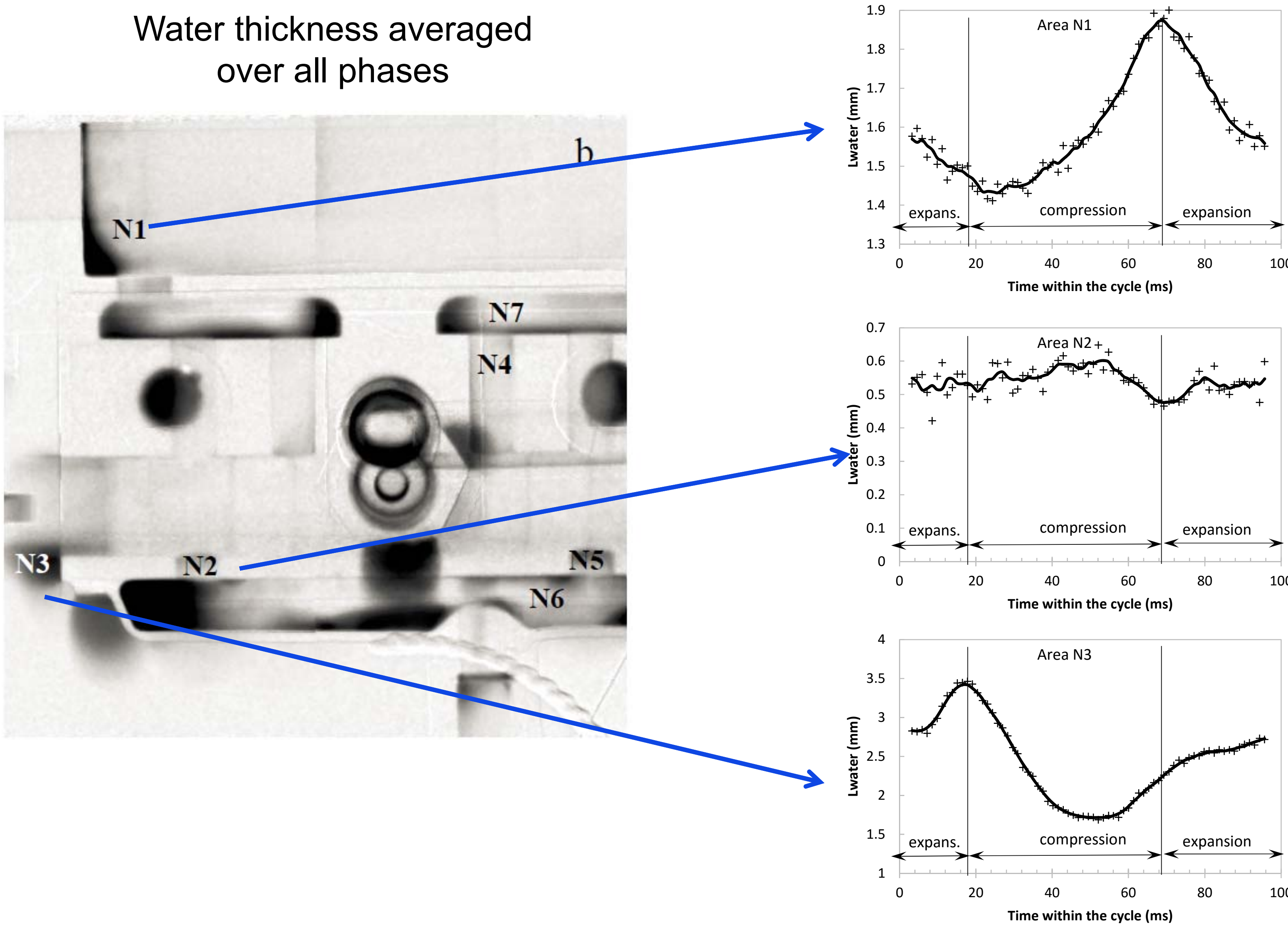

Meteorite studies

Sample 1

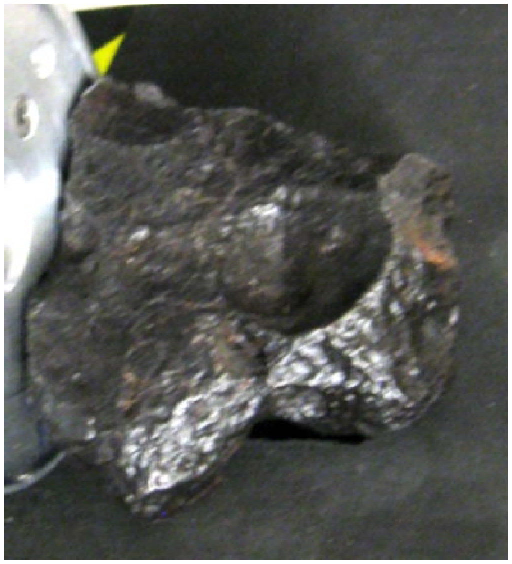

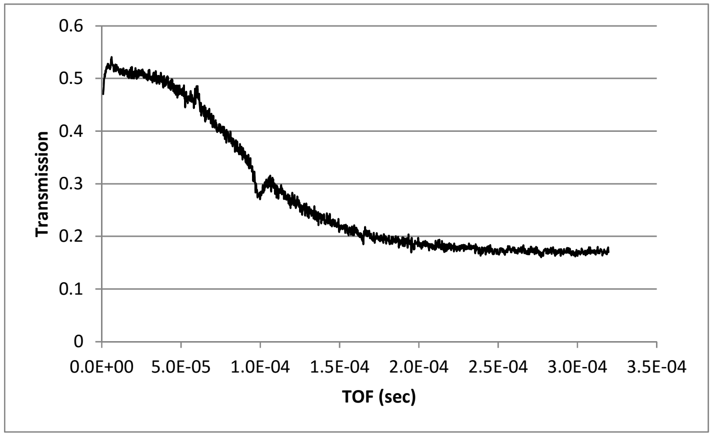

Scan through thermal energies.
$\Delta\lambda/\lambda \sim 0.005$

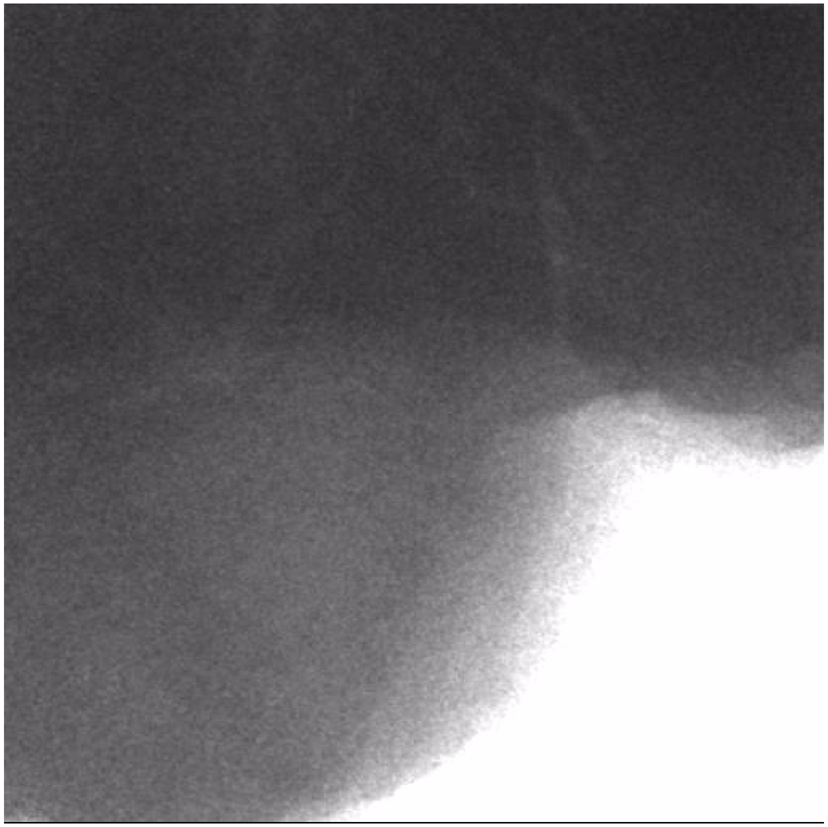

Meteorite studies

Sample 1

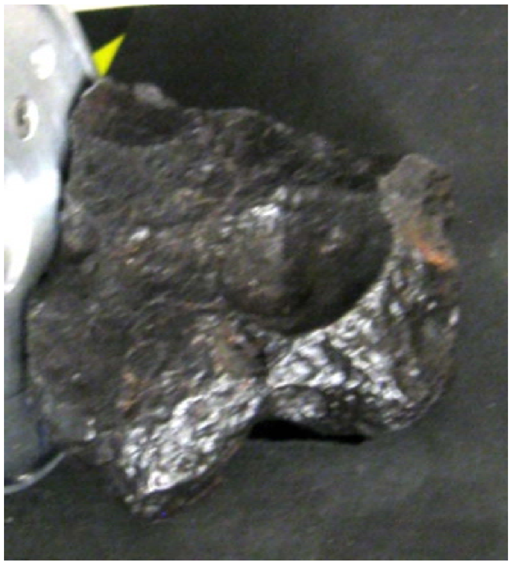

Transmission spectra of different regions

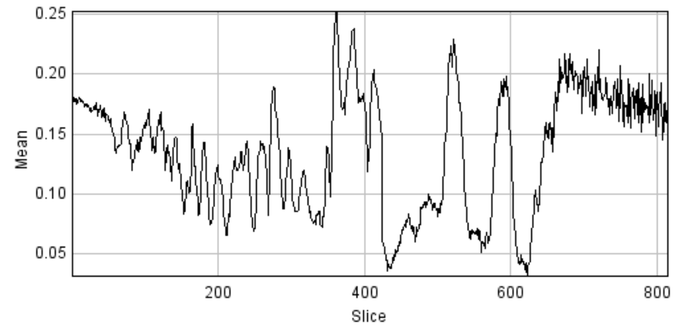

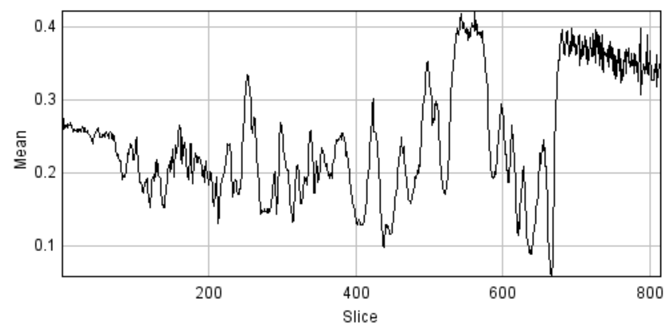

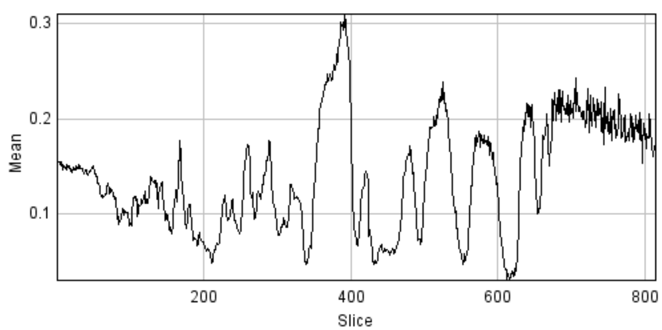

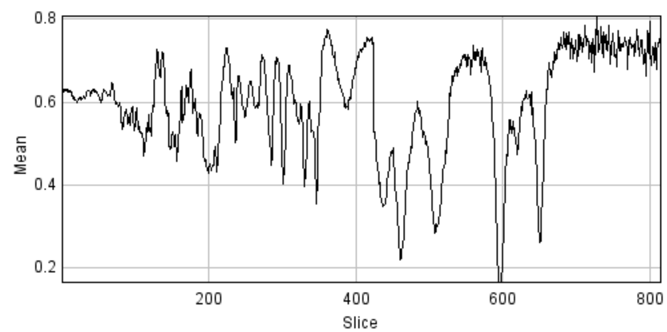

Remote imaging of magnetic field

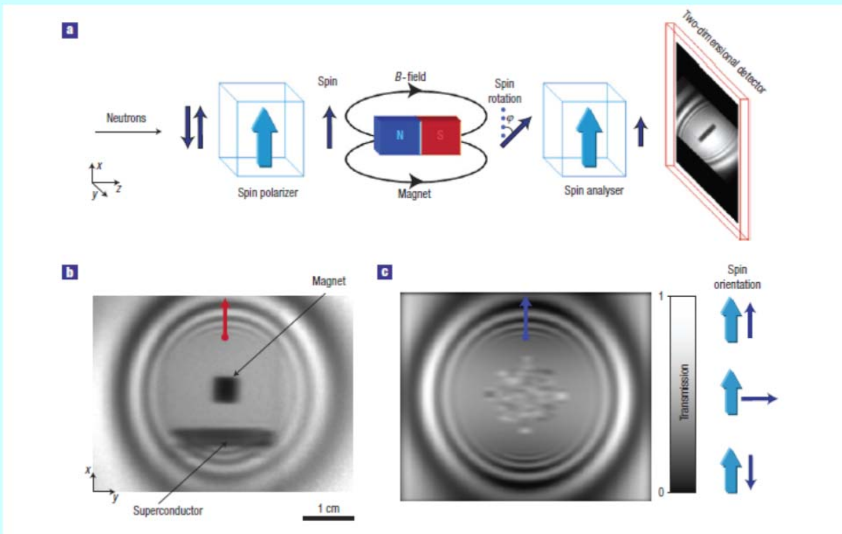

N. Kardjilov et al., Nature Phys. 4 (2008) 399–403

8 μs time slices stacked
into a movie

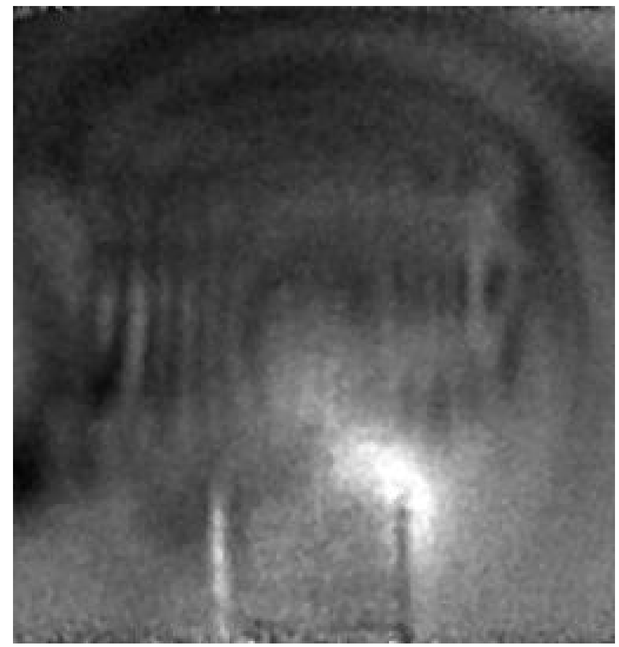

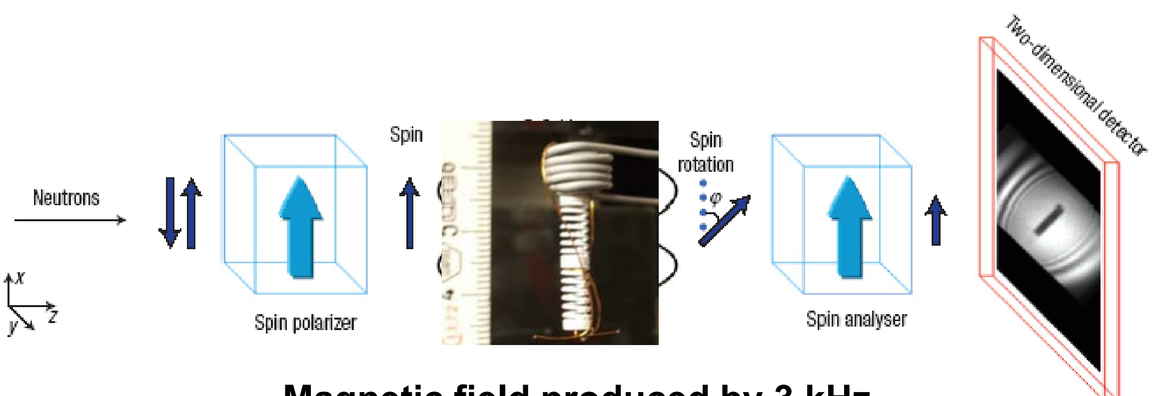

Magnetic field produced by 3 kHz AC current in a coil imaged

[Magnetic Field 3 kHz]

Remote imaging of magnetic field

Images of magnetic field from the coil modeled for different neutron energy

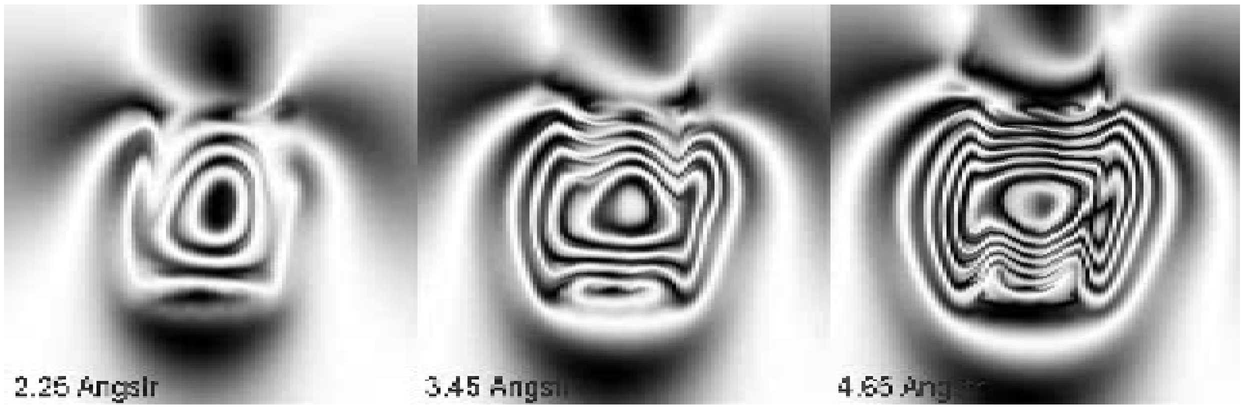

Three neutron energies combined into one image

Measured

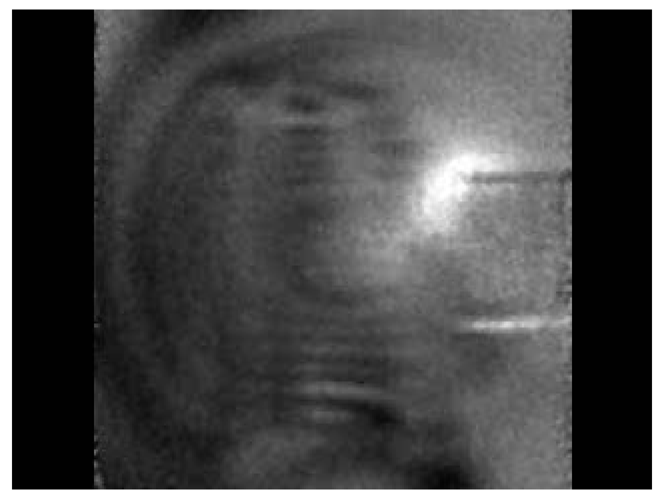

New Journal of Physics 17 (2015) 043047

Summary

- MCP detectors provide unique opportunities in applications where event counting with high spatial and time resolution is required.
- Specific photocathode, type of MCP readout, detector area have to be selected for a particular application.
- Latest developments of MCP manufacturing technology and fast electronics substantially improve the performance of MCP detectors: longer lifetime, high counting rate capabilities, larger sensitive area, many simultaneous particles.
- Various new applications of MCP detectors have been demonstrated recently in very diverse fields.
- These devices are still relatively complicated and not as easy to operate as scientific CCD/CMOS detectors.

This work was supported in part by NASA, DOE, NSF, NIH and NNSA.

The work on MCP/Timepix detector was done within the Medipix collaboration.

Thank you for your attention!